Journal of Machine Learning Research 16 (2015) 1103-1155 Submitted 10/14; Revised 11/14; Published 6/15

Fast Cross-Validation via Sequential Testing

Tammo Krueger TAMMOKRUEGER@GMAIL.COM
Danny Panknin PANKNIN@CS.TU-BERLIN.DE
Mikio Braun MIKIO.BRAUN@TU-BERLIN.DE
Technische Universität Berlin
Machine Learning Group
Marchstr. 23, MAR 4-1
10587 Berlin, Germany

Editor: Charles Elkan

Abstract

With the increasing size of today's data sets, finding the right parameter configuration in model selection via cross-validation can be an extremely time-consuming task. In this paper we propose an improved cross-validation procedure which uses nonparametric testing coupled with sequential analysis to determine the best parameter set on linearly increasing subsets of the data. By eliminating underperforming candidates quickly and keeping promising candidates as long as possible, the method speeds up the computation while preserving the power of the full cross-validation. Theoretical considerations underline the statistical power of our procedure. The experimental evaluation shows that our method reduces the computation time by a factor of up to 120 compared to a full cross-validation with a negligible impact on the accuracy.

Keywords: cross-validation, statistical testing, nonparametric methods

1. Introduction

Model selection by cross-validation is a de-facto standard in applied machine learning to tune parameter configurations of machine learning methods in supervised learning settings (see Mosteller and Tukey 1968; Stone 1974; Geisser 1975 and also Arlot et al. 2010 for a recent and extensive review of the method). Part of the data is held back and used as a test set to get a less biased estimate of the true generalization error. Cross-validation is computationally quite demanding, though. Doing a full grid search on all possible combinations of parameter candidates quickly takes a lot of time, even if one exploits the obvious potential for parallelization.

Therefore, cross-validation is seldom executed in full in practice, but different heuristics are usually employed to speed up the computation. For example, instead of using the full grid, local search heuristics may be used to find local minima in the test error (see for instance Kohavi and John 1995; Bengio 2000; Keerthi et al. 2006). However, in general, as with all local search methods, no guarantees can be given as to the quality of the found local minima. Another frequently used heuristic is to perform the cross-validation on a subset of the data, and then train on the full data set to get the most accurate predictions. The problem here is to find the right size of the subset: If the subset is too small and cannot reflect the true complexity of the learning problem, the configurations selected by cross-validation will lead to underfitted models. On the other hand, a too large subset will take longer for the cross-validation to finish.

Effective use of model selection heuristics requires both an experienced practitioner and familiarity with the data set. However, as we will discuss in more depth below, the effect of taking subsets on the estimated generalization error is more manageable: Given increasing subsets of the data, the test errors converge to the values on the full data set for each parameter configuration, but the parameter configuration achieving the minimum test error will converge much faster. Thus, using subsets in a systematic way opens up a promising way to speed up the model selection process, since training models on smaller subsets of the data is much more time-efficient. During this process care has to be taken when an increase in available data suddenly reveals more structure in the data, leading to a change of the optimal parameter configuration. Still, as we will discuss in more depth, there are ways to guard against such change points, making the heuristic of taking subsets a more promising candidate for an automated procedure.

In this paper we will propose a method which speeds up cross-validation by considering subsets of increasing size. By removing clearly underperforming parameter configurations on the way this leads to a substantial saving in total computation time as sketched in Figure 1. In order to account for possible change points, sequential testing (Wald, 1947) is adapted to control a *safety zone*, roughly speaking, a certain number of allowed failures for a parameter configuration; at the same time this framework allows for dropping clearly underperforming configurations. Finally, we add a stopping criterion to watch for early convergence of the process to further speed up the computation. The resulting method thus consumes less time and space than a full grid cross-validation procedure at no significant loss in accuracy. We prove certain theoretical properties about its optimality, yet, this procedure relies on the availability of a vast amount of data to guide the decision process into a stable region where each configuration sees enough data to show its real performance.

In the following, we will first discuss the effects of taking subsets on learners and cross-validation (Section 2), discuss related work in Section 3, present our method Fast Cross-Validation via Sequential Testing (CVST, Section 4), state the theoretical properties of the method (Section 5) and finally evaluate our method on synthetic and real-world data sets in Section 6. Section 7 gives an overview of possible extensions and Section 8 concludes the paper. The impatient practitioner may skip some theoretical treatments and focus on the self-contained Section 4 describing the CVST algorithm and its evaluation in Section 6. To ease the reading process we collected our notational conventions in Table 1.

2. Cross-Validation on Subsets

Our approach is based on taking subsets of the data to speed up cross-validation. For this approach to work well, we need that the minima of the test errors give reliable estimates of the true performance already for small subsets. In this section, we will discuss the setting and motivate our approach. The goal is to understand which effects lead to making the estimates reliable.

Let us first introduce some notation: Assume that our N training data points d_i are given by input/output pairs $d_i = (X_i, Y_i) \in \mathcal{X} \times \mathcal{Y}$ drawn i.i.d. from some probability

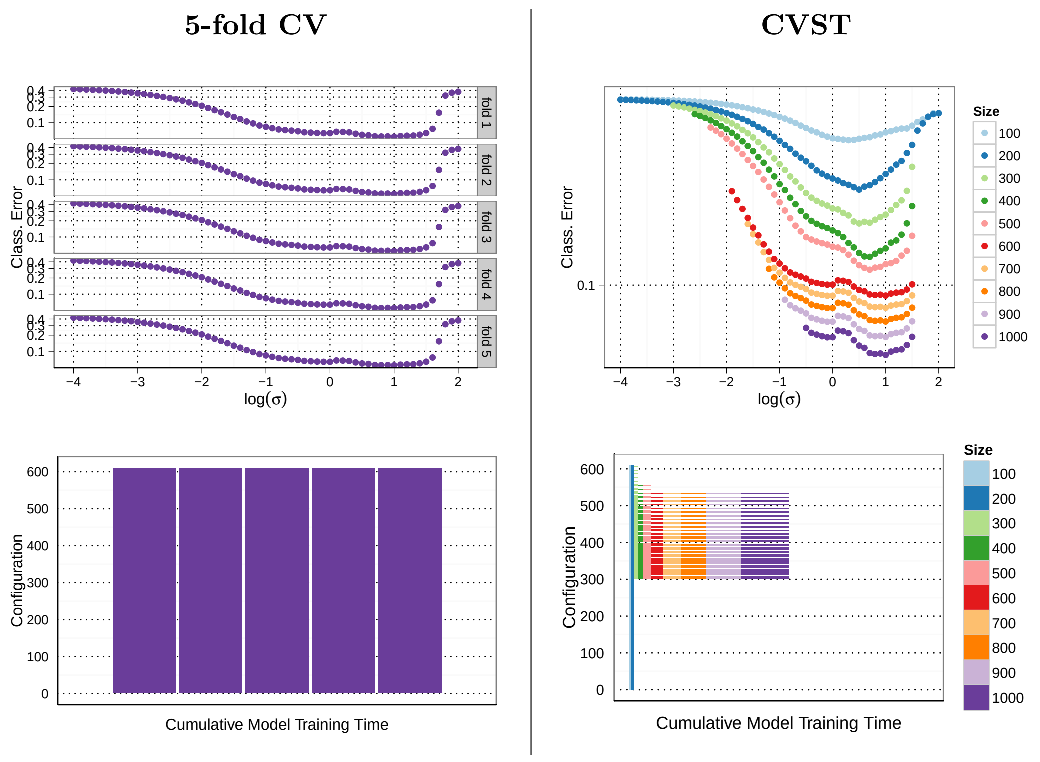

Figure 1: Performance of a 5-fold cross-validation (CV, left) and fast cross-validation via sequential testing (CVST, right): While the CV has to calculate the model for each configuration (here: σ of a Gaussian kernel) on the full data set, the CVST algorithm uses increasing subsets of the data and drops significantly underperforming configurations in each step (upper panels), resulting in a drastic decrease of total calculation time (sum of colored area in lower panels).

distribution P on $\mathcal{X} \times \mathcal{Y}$. We assume an example-wise loss function $\ell\colon \mathcal{Y} \times \mathcal{Y} \to \mathbb{R}$ so that the overall error or expected risk of a predictor $g\colon \mathcal{X} \to \mathcal{Y}$ is given by $R(g) = E[\ell(g(X), Y)]$ where $(X, Y) \sim P$. For some finite set of possible parameter configurations C, let $g_n(c)$ be the predictor learned for parameter $c \in C$ from the first n training examples.

The core procedure in a cross-validation approach is to train predictors for each c and consider their test error. Denote by $g_n(c)$ the predictor obtained by training on the first n points of the training data for parameter c. We wish to study whether this error converges as n grows. Let us denote by c_n^* a configuration optimal for subset size n:

$$R(g_n(c_n^*)) = \min_{c \in C} R(g_n(c)).$$

We will ignore cases where there are multiple minima c_n^*, because we are only interested in the test error achieved, not the location of the minimum.

Symbol	**Description**
$d_i = (X_i, Y_i) \in \mathcal{X} \times \mathcal{Y}$	Data points
N	Total data set size
$g : \mathcal{X} \mapsto \mathcal{Y}$	Learned predictor
$\ell : \mathcal{Y} \times \mathcal{Y} \mapsto \mathbb{R}$	Loss function
$R(g) = E[\ell(g(X), Y)]$	Risk of predictor g
c	Configuration of learner
C	Finite set of examined configurations
$g_n(c) : \mathcal{X} \mapsto \mathcal{Y}$	Predictor learned on n data points for configuration c
c^*	Overall best configuration
c^*_n	Best configuration for models based on n data points
s	Current step of CVST procedure
S	Total number of steps
$\Delta = N/S$	Increment of model size
P_p	Pointwise performance matrix
P_S	Overall performance matrix of dimension $\lvert C\rvert \times S$
T_S	Trace matrix of dimension $\lvert C\rvert \times S$
w_{stop}	Size of early stopping window
$\alpha, \alpha_l, \beta_l$	Significance levels
π	Success probability of a binomial variable

Table 1: List of symbols

In cross-validation, the true test error is not known and estimated by the empirical error on an independent test set. For the sake of simplicity, we will consider the true test error nevertheless for the remainder of this section. In our experience, the effects discussed below also hold for cross-validation, because the estimation error is small and does not create a systematic distortion of the choice of configuration.

Since we want to infer the performance of the predictor on the full training set based on its performance on a subset, we need that the errors are similar for a fixed configuration c as the size of the subset approaches the full training set size. A necessary condition for this to hold in general is that $R(g_n(c))$ converges as n tends to infinity. Luckily, this holds for most existing learning methods (see Appendix A for some examples). A counter example is the case of k-nearest neighbor with fixed k. Training with $k = 10$ leads to quite different predictions on data sets of size 100 compared to, say, 10,000. More discussion can be found below in Section 5.3.

We are interested in the difference in errors between the best parameter configuration learned on the subset of size n, and on the full data set N, that is, $R(g_n(c^*_n)) - R(g_N(c^*_N))$. This error can be bounded by considering the difference between $R(g_n(c))$ and $R(g_N(c))$ uniformly over the whole configuration set C. If the learner itself converges it is trivial to show that the errors also converge for finite parameter configuration sets C. On the other hand, uniform convergence is quite a strong requirement, since it requires that the test errors also converge for suboptimal configurations. In particular for parameter configurations c

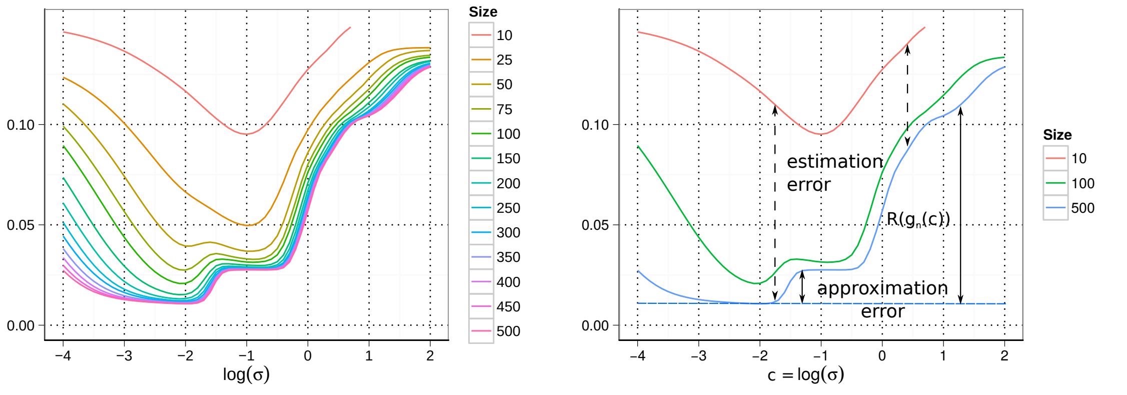

(a) (b)

Figure 2: Test error of an SVR model on the *noisy sinc* data set introduced in Section 6.1. We can observe a shift of the optimal σ of the Gaussian kernel to the fine-grained structure of the problem, if we have seen enough data. In Figure (b), approximation error is indicated by the black solid line, and the estimation error by the black dashed line. The minimal risk is shown as the blue dashed line. One can see that uniform approximation of the estimation error is not the main driving force, instead, the decay of the approximation error with smaller kernel widths together with an increase of the estimation error at small kernel widths makes sure that the minimum converges quickly.

which correspond to complex models, $g_n(c)$ may continue to improve right up to the full number N of data points.

So while uniform convergence seems a sufficient condition, let us look at a concrete example to see whether uniform convergence is a necessary condition for convergence of the minima. Figure 2(a) shows the test errors for a typical example. We train a support vector regression model (SVR) on subsets of the full training set consisting of 500 data points. The data set is the *noisy sinc* data set introduced in Section 6.1. Model parameters are the kernel width σ of the Gaussian kernel used and the regularization parameter, where the results shown are already optimized over the regularization parameter for the sake of simplicity.

We see that the minimum converges rather quickly, first to the plateau of $\log(\sigma) \in [-1.5, -0.3]$ approximately, and then towards the lower one at $[-2.5, -1.7]$, which is also the optimal one at training set size $n = 500$. We see that uniform convergence is not the main driving force. In fact, the errors for small kernel widths are still very far apart even when the minimum is already converged.

In the following, it is helpful to continue the discussion using the concepts of estimation error and approximation error. We assume that the learner is trained by picking the model which minimizes the empirical risk over some hypothesis set $\mathcal{G}$. Let us denote this predictor as g_n^*. In this setting, one can write the difference between the expected risk of the predictor $R(g_n^*)$ and the Bayes risk R^* as follows (see Section 12.1 in Devroye et al. 1996 or

Section 2.4.3 in Mohri et al. 2012):

$$R(g_n^*) - R^* = \underbrace{\left(R(g_n^*) - \inf_{g\in\mathcal{G}} R(g)\right)}_{\text{estimation error}} + \underbrace{\left(\inf_{g\in\mathcal{G}} R(g) - R^*\right)}_{\text{approximation error}}.$$

The estimation error measures how far the chosen model is from the one which would be asymptotically optimal, while the approximation error measures the difference in risk between the best possible model in the hypothesis class and the true function.

Using this decomposition, we can interpret the figure as follows (see Figure 2(b)): The kernel width controls the approximation error. For $\log(\sigma) \geq -1.8$, the resulting hypothesis class is too coarse to represent the function under consideration. It becomes smaller until it reaches the level of the Bayes risk as indicated by the dashed blue line. For even larger training set sizes, we can assume that it will stay on this level even for smaller kernel sizes.

The difference between the blue line and the upper lines shows the estimation error. The estimation error has been extensively studied in statistical learning theory and is known to be linked to different notions of complexity like VC-dimension (Vapnik, 1998), fat-shattering dimension (Bartlett et al., 1996), or the norm in the reproducing kernel Hilbert space (RKHS) (Evgeniou and Pontil, 1999). A typical result shows that the estimation error can be bounded by terms of the form

$$R(g_n^*) - \inf_{g\in\mathcal{G}} R(g) \leq O\left(\sqrt{\frac{d(\mathcal{G})\log n}{n}}\right),$$

where $d(\mathcal{G})$ is some notion of complexity of the underlying hypothesis class, and the bound holds with high probability. For our figure, this means that we can expect the estimation error to become larger for smaller kernel widths.

If we image the parameter configurations ordered according to their complexity, we see that for parameter configurations with small complexity (that is, large kernel width), the approximation error will be high, but the estimation error will be small. At the same time, for parameter configurations with high complexity, the approximation error will be small, even optimal, but the estimation error will be large, although it will decay with increasing training set size. In combination, the estimates at smaller training set sizes tend to underestimate the true model complexity, but as the estimation error decreases and becomes small compared to the approximation error, the minimum also converges to the true one. The fact that the estimation error is larger for more complex models acts as a guard to choose too complex models. The estimation error for models which have higher complexity than the optimal one can effectively be ignored. Therefore, we can expect much faster convergence than given by a uniform error bound, which is, however, highly data dependent.

Unfortunately, existing theoretical results are not able to bound the error sufficiently tightly to make these arguments more exact. In particular, the speed of the convergence on the minimum hinges on a tight lower bound on the approximation error, and a realistic upper bound on the estimation error. Approximation errors have been studied for example in the papers by Smale and Zhou (2003) and Steinwart and Scovel (2007), but the papers only prove upper bounds, and the rates are also worst-case rates which are likely not close enough to the true errors. A more formal study of the effects discussed above is therefore the subject of future work.

On the other hand, the mechanisms which lead to fast convergence of the minimum are plausible when looking at concrete examples as we did above. Therefore, we will assume in the following that the location of the best parameter configuration might initially change but then become more or less stable quickly. Note that we do not claim that the speed of this convergence is known. Instead, we will use sequential testing to introduce a *safety zone* which will be as large as possible to ensure that our method is robust against these initial changes and good configurations survive till final stable regime.

3. Related Work

Using statistical tests and the sequential analysis framework in order to speed up learning has been the topic of several lines of research. However, the existing body of work mostly focuses on reducing the number of test evaluations, while we focus on the overall process of eliminating candidates themselves. To the best of our knowledge, this is a new concept and can apparently be combined with the already available racing techniques to further reduce the total calculation time.

Maron and Moore (1994, 1997) introduce the so-called *Hoeffding Races* which are based on the nonparametric Hoeffding bound for the mean of the test error. At each step of the algorithm a new test point is evaluated by all remaining models and the confidence intervals of the test errors are updated accordingly. Models whose confidence interval of the test error lies outside of at least one interval of a better performing model are dropped. In a similar vein Zheng and Bilenko (2013) have applied this concept to cross-validation and improve this approach by using paired t-test and power analysis to control both the false positive and false negative rate. Chien et al. (1995, 1999) devise a similar range of algorithms using concepts of PAC learning and game theory: Different hypotheses are ordered by their expected utility according to the test data the algorithm has seen so far. As for Hoeffding Races, the emphasis in this approach lies on reducing the number of evaluations. Thus, the application domain for these kind of algorithms is best suited where the evaluation of a data point given a learned model is costly. Since this approach expects that a model is fully trained before its evaluation, the direct utilization of racing algorithms for model selection would result in a procedure similar to a one-fold cross-validation: First learn a model on one half of the data and do the time efficient evaluation as described above on the other half. Obviously, this would yield a maximal relative time improvement of k compared to standard k-fold cross-validation since we learn one model instead of the k for k-fold cross-validation. Yet, the orthogonality of this approach to the CVST procedure could be utilized in each step and for each remaining configuration to further increase the runtime benefits by minimizing the necessary evaluations of a model for determining whether it belongs to the top configurations or not.

This concept of racing is further extended by Domingos and Hulten (2001): By introducing an upper bound for the learner's loss as a function of the examples, the procedure allows for an early stopping of the learning process, if the loss is nearly as optimal as for infinite data. Birattari et al. (2002) apply racing in the domain of evolutionary algorithms and extend the framework by using the Friedman test to filter out non-promising configurations. While Bradley and Schapire (2008) use similar concepts in the context of boosting (FilterBoost), Mnih et al. (2008) introduce the empirical Bernstein Bounds to extend both the FilterBoost framework and the racing algorithms. In both cases the bounds are used to estimate the error within a specific ϵ-region with a given probability. Pelossof and Jones (2009) use the concept of sequential testing to speed up the boosting process by controlling the number of features which are evaluated for each sample. In a similar fashion this approach is used in Pelossof and Ying (2010) to increase the speed of the evaluation of the perceptron and in Pelossof and Ying (2011) to speed up the Pegasos algorithm. Stanski (2012) uses a partial leave-one-out evaluation of model performance to get an estimate of the overall model performance, which is used to pick the most probable best model. These racing concepts are applied in a wide variety of domains like reinforcement learning (Heidrich-Meisner and Igel, 2009) and timetabling (Birattari, 2009) showing the relevance and practical impact of the topic.

Recently, Bayesian optimization has been applied to the problem of hyper-parameter optimization of machine learning algorithms. Bergstra et al. (2011) use the sequential model-based global optimization framework (SMBO) and implement the loss function of an algorithm via hierarchical Gaussian processes. Given the previously observed history of performances, a candidate configuration is selected which minimizes this historical surrogate loss function. Applied to the problem of training deep belief networks this approach shows superior performance over random search strategies. Snoek et al. (2012) extend this approach by including timing information for each potential model, i.e., the cost of learning a model and optimizing the expected improvement per seconds leads to a global optimization in terms of wall-clock time. Thornton et al. (2012) apply the SMBO framework in the context of the WEKA machine learning toolbox: The so-called Auto-WEKA procedure not only finds the optimal parameter for a specific learning problem but also searches for the most suitable learning algorithm. Like the racing concepts, these Bayesian optimization approaches are orthogonal to the CVST approach and could be combined to speed up each step of the CVST loop.

On first sight, the multi-armed bandit problem (Berry and Fristedt, 1985; Cesa-Bianchi and Lugosi, 2006) also seems to be related to the problem here in another way: In the multi-armed bandit problem, a number of distributions are given and the task is to identify the distribution with the largest mean from a chosen sequence of samples from the individual distributions. In each round, the agent chooses one distribution to sample from and typically has to find some balance between exploring the different distributions, rejecting distributions which do not seem promising and focusing on a few candidates to get more accurate samples.

This looks similar to our setting where we also wish to identify promising candidates and reject underperforming configurations early on in the process, but the main difference is that the multi-armed bandit setting assumes that the distributions are fixed whereas we specifically have to deal with distributions which change as the sample size increases. This leads to the introduction of a safety zone, among other things. Therefore, the multi-armed bandit setting is not applicable across different sample sizes. On the other hand, the multi-armed bandit approach is a possible extension to speed up the computation within a fixed training size similar to the Hoeffding races already mentioned above.

4. Fast Cross-Validation via Sequential Testing (CVST)

Recall from Section 2 that we have a data set consisting of N data points $d_i = (X_i, Y_i) \in \mathcal{X} \times \mathcal{Y}$ which we assume to be drawn i.i.d. from P. We have a learning algorithm which depends on several parameters collected in a configuration $c \in C$. The goal is to select the configuration c^* out of all possible configurations C such that the learned predictor g has the best generalization error with respect to some loss function $\ell : \mathcal{Y} \times \mathcal{Y} \to \mathbb{R}$.

Our approach attempts to speed up the model selection process by learning just on subsamples of size $n := s\frac{N}{S} = s\Delta$ for $1 \leq s \leq S$ where S is the maximal number of steps the CVST algorithm should run. The procedure starts with the full set of configurations and eliminates clearly underperforming configurations at each step s based on the performances observed in steps 1 to s. The main loop of Algorithm 1 on page 1112 executes the following parts at each step s:

❶ The procedure learns a model on the first n data points for the remaining configurations and stores the test errors on the remaining $N - n$ data points in the pointwise performance matrix P_p (Lines 10-14). This matrix P_p is used on Lines 15-16 to estimate the top performing configurations via robust testing (see Algorithm 2) and saves the outcome as a binary "top or flop" scheme accordingly.

❷ The procedure drops significant loser configurations along the way (Lines 17-19 and Algorithm 3) using tests from the sequential analysis framework.

❸ Applying robust, distribution free testing techniques allows for an early stopping of the procedure when we have seen enough data for a stable parameter estimation (Line 20 and Algorithm 4).

In the following we will discuss the individual steps in the algorithm and formally define the notations used. A conceptual overview of one iteration of the procedure is depicted in Figure 3 for reference. Additionally, we have released a software package on CRAN named `CVST` which is publicly available via all official CRAN repositories and also via GitHub (`https://github.com/tammok/CVST`). This package contains the CVST procedure and all learners used in Section 6 ready for use.

4.1 Robust Transformation of Test Errors

To robustly transform the performance of configurations into the binary information whether it is among the top-performing configurations or turns out to be a flop, we rely on distribution-free tests. The basic idea is to calculate the performance of a given configuration on data points not used during learning and store this information in the pointwise performance matrix P_p. Then we find the group of best configurations by first ordering them according to their mean performance in this step and then compare in a stepwise fashion whether the pointwise performance matrix P_p of a given subset of the configurations are significantly different.

We give an example of this procedure by the situation depicted in Figure 3 with K remaining configurations $c_1, c_2, \ldots, c_K$ which are ordered according to their mean performances (i.e., sorted ascending with regard to their expected loss). We now want to find the

Algorithm 1 CVST Main Loop

```
1: function CVST($d_1, \dots, d_N$, $S$, $C$, $\alpha$, $\beta_l$, $\alpha_l$, $w_{\text{stop}}$)
2:     $\Delta \leftarrow \text{N}/S$                                        ▷ Initialize subset increment
3:     $n \leftarrow \Delta$                                                 ▷ Initialize model size
4:     test ←getTest($S$, $\beta_l$, $\alpha_l$)                            ▷ Get sequential test
5:     $\forall \text{s} \in \{1, \dots, S\}, c \in C : T_S[c, s] \leftarrow 0$
6:     $\forall \text{s} \in \{1, \dots, S\}, c \in C : P_S[c, s] \leftarrow \text{NA}$
7:     $\forall c \in C$ : isActive[$c$] ←**true**
8:     for $s \leftarrow 1$ to $S$ do
9:         $\forall \text{i} \in \{1, \dots, N-n\}, c \in C : P_p[c, i] \leftarrow \text{NA}$
10:        for $c \in C$ do
11:            if isActive[$c$] then
12:                $g = g_n(c)$                          ▷ Learn model on the first $n$ data points
13:                $\forall i \in \{1, \dots, N-n\} : P_p[c, i] \leftarrow \ell(g(x_{n+i}), y_{n+i})$     ▷ Evaluate on the rest
14:                $P_S[c, s] \leftarrow \frac{1}{N-n} \sum_{i=1}^{N-n} P_p[c, i]$          ▷ Store mean performance
15:        index$_{\text{top}}$ ←topConfigurations($P_p, \alpha$)          ▷ Find the top configurations
16:        $T_S$[index$_{\text{top}}$, $s$] ←1                             ▷ And set entry in trace matrix
17:        for $c \in C$ do
18:            if isActive[$c$] and isFlopConfiguration($T_S[c, 1 : s]$, s, $S$, $\beta_l$, $\alpha_l$) then
19:                isActive[c] ←**false**                      ▷ De-activate flop configuration
20:        if similarPerformance($T_S$[isActive, $(s - w_{\text{stop}} + 1) : s$], $\alpha$) then
21:            break
22:        $n \leftarrow n + \Delta$
23:    return selectWinnner($P_S$, isActive, $w_{\text{stop}}$, $s$)
```

Algorithm 2 Find the top configurations via iterative testing

```
1: function topConfigurations($P_p, \alpha$)
2:     $\forall i \in \{1, \dots, C\} : P_m[k] \leftarrow \frac{1}{N-n} \sum_{j=1}^{N-n} P_p[k, j]$
3:     index$_{\text{sort}}$ ← sortIndexDecreasing($P_m$)
4:     $\widetilde{P}_p = P_p[\text{index}_{\text{sort}}, ]$                 ▷ Sort $P_p$ according to the mean performance
5:     $K$ ←which(isNA($P_m$)) $- 1$                    ▷ $K$ is the number of active configurations
6:     $\tilde{\alpha} = \alpha/(K-1)$                 ▷ Bonferroni correction for $K-1$ potential tests
7:     for $k \in \{2, \dots, K\}$ do
8:         if is classification task then                          ▷ Choose according test
9:             $p \leftarrow$ cochranQTest($\widetilde{P}_p[1 : k, ]$)
10:        else
11:            $p \leftarrow$ friedmanTest($\widetilde{P}_p[1 : k, ]$)
12:        if $p \leq \tilde{\alpha}$ then                                ▷ We found a significant effect
13:            break              ▷ so the $k - 1^{\text{th}}$ preceding configurations are the top ones
14:    return index$_{\text{sort}}[1 : (k-1)]$
```

Algorithm 3 Check for flop configurations via sequential testing

```
1: function isFlopConfiguration($T$, s, $S$, $\beta_l$, $\alpha_l$)
2:     $\pi_0 \leftarrow 0.5; \pi_1 \leftarrow \frac{1}{2}\sqrt[S]{\frac{1-\beta_l}{\alpha_l}}$
3:     $a \leftarrow \frac{\log \frac{\beta_l}{1-\alpha_l}}{\log \frac{\pi_1}{\pi_0} - \log \frac{1-\pi_1}{1-\pi_0}}$
4:     $b \leftarrow \frac{\log \frac{1-\pi_0}{1-\pi_1}}{\log \frac{\pi_1}{\pi_0} - \log \frac{1-\pi_1}{1-\pi_0}}$
5:     return $\sum_{i=1}^{s} T_i \leq a + bs$
```

Algorithm 4 Compare performance of remaining configurations

```
1: function similarPerformance($T_S$, $\alpha$)
2:     $p \leftarrow$ cochranQTest($T_S$)
3:     return $p \leq \alpha$
```

smallest index $k \leq K$, such that the configurations $c_1, c_2, \dots, c_k$ all show a similar behavior on the remaining data points $d_{n+1}, d_{n+2}, \dots, d_N$ not used in the current model learning process based on a statistical test.

The rationale behind our comparison procedure is three-fold: First, by ordering the configurations by the mean performances we start with the comparison of the currently best performing configurations first. Second, by using the first $n := s\Delta$ data points for the model building and the remaining $N - n$ data points for the estimation of the average performance of each configuration, we compensate the error introduced by learning on smaller subsets of the data by better error estimates on more data points. I.e., for small s we will learn the model on relatively small subsets of the overall available data while we estimate the test error on relatively large portions of the data and vice versa. Third, by applying test procedures directly on the error estimates of individual data points we exploit a further robustifying pooling effect: If we have outliers in the testing data, all models will be affected by this and therefore the overall testing result will not be affected. We will

Algorithm 5 Select the winning configuration out of the remaining ones

```
1: function selectWinnner($P_S$, isActive, $w_{\text{stop}}$, $s$)
2:     $\forall$i $\in \{1, \dots, s\}, c \in C : R_S[c, i] \leftarrow \infty$
3:     for $i \in \{1, \dots, s\}$ do
4:         for $c \in C$ do
5:             if isActive[$c$] then
6:                 $R_S[c, i] = \text{rank}(P_S[c, i], P_S[, i])$        ▷ Gather the rank of $c$ in step $i$
7:     $\forall c \in C : M_S[c] \leftarrow \infty$
8:     for $c \in C$ do
9:         if isActive[$c$] then
10:            $M_S[c] \leftarrow \frac{1}{w_{\text{stop}}} \sum_{i=s-w_{\text{stop}}+1}^{s} R_S[c, i]$        ▷ Mean rank for the last $w_{\text{stop}}$ steps
11:    return whichMin($M_S$)        ▷ Return configuration with minimal mean rank
```

	data points						
conf.	d_{n+1}	d_{n+2}	$\cdots$	d_{N-1}	d_N	$E[\ell]$	
c_1	0.6	0.6		-0.8	-0.4	0.5	top
c_2	0.5	0.4		-0.3	0.0	0.5	top
c_3	0.1	0.5	$\cdots$	-0.9	-0.1	0.6	top
$\vdots$		$\vdots$		$\vdots$		$\vdots$	
c_{K-2}	-1.4	-0.9		0.5	0.5	1.5	flop
c_{K-1}	-2.2	-1.9		2.1	1.5	1.5	flop
c_K	-1.9	-2.4	$\cdots$	1.9	2.4	1.6	flop

Pointwise performance matrix P_p

❶ $\rightarrow$

step										
1	2	3	4	5	6	7	8	9	10	
0	1	0	1	1	1	1	0	1	1	
1	1	0	1	1	1	0	1	1	1	
0	1	1	1	1	1	0	1	1	1	
					$\vdots$					
0	1	1	0	0	1	0	0	0	0	
0	0	0	0	1	0	0	0	0	0	(†)
0	1	0	0	0	0	0	0	0	0	(†)

Trace matrix T_S

❷ $\swarrow$

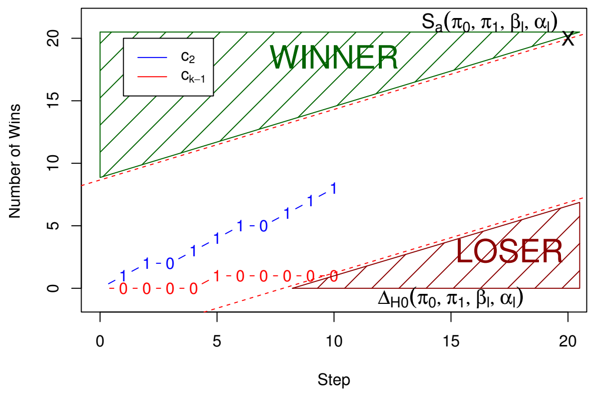

❸ $\downarrow$

	7	8	9	10
c_1	1	0	1	1
c_2	0	1	1	1
c_3	0	1	1	1
$\vdots$		$\vdots$		
c_{K-2}	0	0	0	0

$\overset{?}{=}$

SIMILARPERFORMANCE$(\cdot)$

Figure 3: One step of CVST. Shown is the situation in step $s = 10$. ❶ A model based on the first n data points is learned for each configuration (c_1 to c_K). Test errors are calculated on the remaining data (d_{n+1} to d_N) and transformed into a binary performance indicator via robust testing. ❷ Traces of configurations are filtered via sequential analysis (c_{K-1} and c_K are dropped). ❸ The procedure checks whether the remaining configurations perform equally well in the past and stops if this is the case. See Appendix B for a complete example run.

see in the evaluation section that all these effects are indeed helpful for an overall good performance of the CVST algorithm.

To find the top performing configurations for step s we look at the outcome of the learned model for each configuration, i.e., we subsequently take the rows of the pointwise performance matrix P_p into account and apply either the Friedman test (Friedman, 1937) for regression experiments or the Cochran's Q test (Cochran, 1950) to see whether we observe statistically significant differences between configurations (see Appendix C for a summary of these tests). In essence these robust tests check whether the performance outcomes of a subset of the configurations show significant differences, i.e., in our case behave differently in terms of overall best performance. The assumption here is that the mean performance of a configuration is a good, yet wiggly estimator of its overall performance. By subsequently checking the finer-grained outcome of the models on the individual data points we want to find the breakpoint where the overall top-performing configurations for this step are separated from the rest of the configurations which will show a significantly different behavior on the individual data points.

More formally, the function topConfigurations described in Algorithm 2 takes the pointwise performance matrix P_p as input and rearranges the rows according to the mean performances of the configurations yielding a matrix $\widetilde{P}_p$. Now for $k \in \{2, 3, \ldots, K\}$ we check, whether the first k configurations show a significantly different effect on the $N - n$ data points. This is done by executing either the Friedman test or the Cochran's Q test on the submatrix $\widetilde{P}_p[1 : k, 1 : (N-n)]$ with the pre-specified significance level α. If the test does not indicate a significant difference in the performance of the k configurations, we increment k by one and test again until we find a significant effect. Suppose we find a significant effect at index $\tilde{k}$. Since all previous tests indicated no significant effect for the $\tilde{k}-1$ configurations we argue that the addition of the $\tilde{k}^{\text{th}}$ configuration must have triggered the test procedure to indicate that in the set of these $\tilde{k}$ configurations is at least one configuration, which shows a significantly different behavior than all other configurations. Thus, we flag the configurations $1, \ldots, \tilde{k} - 1$ as top configurations and the remaining $\tilde{k}, \ldots, K$ configurations as flop configurations. Note that this incremental procedure is a multiple testing situation, thus we apply the Bonferroni correction to the calculated p-values.

For the actual calculation of the test errors we apply an incremental model building process, i.e., the data added in each step on Line 22 increases the training data pool for each step by a set of size Δ. This would allow online algorithms to adapt their model also incrementally leading to even further speed improvements. The results of this first step are collected for each configuration in the trace matrix T_S (see Figure 3, top right), which shows the gradual transformation for the last 10 steps of the procedure highlighting the results of the last test. More formally, $T_S[c, s]$ is 1 iff configuration c is amongst the top configuration in step s; if c is not a top configuration in step s, the entry $T_S[c, s]$ is 0.

So this new column generated in step s in the trace matrix T_S summarizes the performance of all models learned on the first n data points in a robust way. Thus, the trace matrix T_S records the history of each configuration in a binary fashion, i.e., whether it performed as a top or flop configuration in each step of the CVST main loop. This leads to a robust transformation of the test errors of the configurations which can be modeled in the next step as a binary random variable with a success probability π indicating whether a configuration is amongst the top (high π) or the flop (low π) configurations.

4.2 Determining Significant Losers

Having transformed the test errors in a scale-independent top or flop scheme, we can now test whether a given parameter configuration is an overall loser. For this we represent a configuration as a binary random variable which turns out to be a top configuration with a given probability π. During the course of the execution of the CVST algorithm we gather information about the behavior of each configuration and want to estimate at each step whether the observed behavior is more likely to be associated with a binomial variable having a high π meaning that it is a winning configuration or a low one deeming it as a loser configuration. The standard tool for this kind of task is the sequential testing of binary random variables which is addressed in the *sequential analysis* framework developed by Wald (1947). Originally it has been applied in the context of production quality assessment (compare two production processes) or biological settings (stop bioassays as soon as the gathered data leads to a significant result). In this section we focus on the general idea of this approach while Section 5 gives details about how the CVST algorithm deals with potential switches in the winning probability π of a given configuration.

The main idea of the sequential analysis framework is the following: One observes a sequence of i.i.d. Bernoulli variables $B_1, B_2, \ldots$, and wants to test whether these variables are distributed according to the hypotheses $H_0 : B_i \sim \pi_0$ or the alternative hypotheses $H_1 : B_i \sim \pi_1$ with $\pi_0 < \pi_1$ denoting the according success probabilities of the Bernoulli variables. Both significance levels for the acceptance of H_1 and H_0 can be controlled via the user-supplied meta-parameters α_l and β_l. The test computes the likelihood for the so far observed data and rejects one of the hypothesis when the respective likelihood ratio exceeds an interval controlled by the meta-parameters. It can be shown that the procedure has a very intuitive geometric representation, shown in Figure 3, lower left: The binary observations are recorded as cumulative sums at each time step. If this sum exceeds the upper red line L_1, we accept H_1; if the sum is below the lower red line L_0 we accept H_0; if the sum stays between the two red lines we have to draw another sample.

Wald's test requires that we fix both success probabilities π_0 and π_1 beforehand. Since our main goal is to use the sequential test to eliminate underperformers, we choose the parameters π_0 and π_1 of the test such that H_1 (a configuration wins) is postponed as long as possible. This will allow the CVST algorithm to keep configurations until the evidence of their performances definitely shows that they are overall loser configurations. At the same time, we want to maximize the area where configurations are eliminated (region $\triangle_{H_0}$ denoted by "LOSER" in Figure 3), rejecting as many loser configurations on the way as possible:

$$\begin{aligned}(\pi_0, \pi_1) \quad &= \quad \underset{\pi_0', \pi_1'}{\operatorname{argmax}} \; \triangle_{H_0}(\pi_0', \pi_1', \beta_l, \alpha_l) \\ &\quad\quad \text{s.t. } S_a(\pi_0', \pi_1', \beta_l, \alpha_l) \in (S-1, S]\end{aligned} \tag{1}$$

with $S_a(\cdot,\cdot,\cdot,\cdot)$ being the earliest step of acceptance of H_1 marked by an X in Figure 3 and S denotes again the total number of steps. By using approximations from Wald (1947) for the expected number of steps the test will take, if the real success probability of the underlying process would indicate a constant winner (i.e., $\pi = 1.0$), we can fix S_a to the maximal number of steps S and solve Equation (1) as follows (see Appendix D for details):

$$\pi_0 = 0.5 \wedge \pi_1 = \frac{1}{2}\sqrt[S]{\frac{1-\beta_l}{\alpha_l}}. \tag{2}$$

Equipped with these parameters for the sequential test, we can check each remaining trace on Line 18 of Algorithm 1 in the function isFlopConfiguration detailed in Algorithm 3 whether it is a statistically significant flop configuration (i.e., exceeds the lower decision boundary L_0) or not.

Note that sequential analysis formally requires i.i.d. variables. In the CVST procedure both the independence of the top/flop variable and the identically distributed assumption might be violated for configurations which transform to a winner configuration later on, thereby changing their behavior from a flop to a top configuration. With the modeling approach taken in this step of the CVST algorithm this would amount to a change of the underlying success probability π of the configuration. Thus, the assumptions of the sequential testing framework would definitely be violated. We accommodate for this by introducing in Section 5.1 a so-called *safety zone* which acts as a safeguard against prematurely dropping of a configuration. Note that this safety zone can be controlled by the experimenter using the parameters α_l and β_l of the sequential test. If the experimenter chooses the right safety zone the underlying success probabilities of the configuration remain stable after the safety zone and, hence, again will satisfy the preconditions of the sequential testing framework. So by ensuring no premature drop of a configuration in the safety zone we heuristically adapt the sequential test to the potential switch of underlying success probabilities. To give a complete account of the assumptions of the sequential analysis we will discuss potential violations of the independence of the top/flop variables and its implication for the CVST procedure in Section 5.

For details of the open sequential analysis please consult Wald (1947) or see for instance Wetherill and Glazebrook (1986) for a general overview of sequential testing procedures. Appendix D contains the necessary details needed to implement the proposed testing scheme for the CVST algorithm.

4.3 Early Stopping and Final Winner

Finally, we employ an early stopping rule (Line 20) which takes the last w_{stop} columns from the trace matrix and checks whether all remaining configurations performed equally well in the past. In Figure 3 this submatrix of the overall trace matrix T_S is shown for a value of $w_{\text{stop}} = 4$ for the remaining configurations after step 10. For the test, we again apply the Cochran's Q test (see Appendix C) in the similarPerformance procedure on the submatrix of T_S as denoted in Algorithm 4. Figure 4 illustrates a complete run of the CVST algorithm for roughly 600 configurations. Each configuration marked in red corresponds to a flop configuration and a black one to a top configuration. Configurations marked in gray have been dropped via the sequential test during the CVST algorithm. The small zoom-ins in the lower part of the picture show the last w_{stop} remaining configurations during each step which are used in the evaluation of the early stopping criterion. We can see that the procedure keeps on going if there is a heterogeneous behavior of the remaining configurations (zoom-in is mixed red/black). When all the remaining configurations performed equally well in the past (zoom-in is nearly black), the early stopping test does not see a significant effect anymore and the procedure is stopped.

Finally, in the procedure selectWinner, Line 23 and Algorithm 5, the winning configuration is picked from the configurations which have survived all steps as follows: For each remaining configuration we determine the rank in a step according to the average performance during this step. Then we average the rank over the last w_{stop} steps and pick the configuration which has the lowest mean rank. This way, we make most use of the data accumulated during the course of the procedure. By restricting our view to the last w_{stop} observations we also take into account that the optimal parameter might change with increasing model size: Since we focus on the most recent observations with the biggest models, we always pick the configuration which is most suitable for the data size at hand.

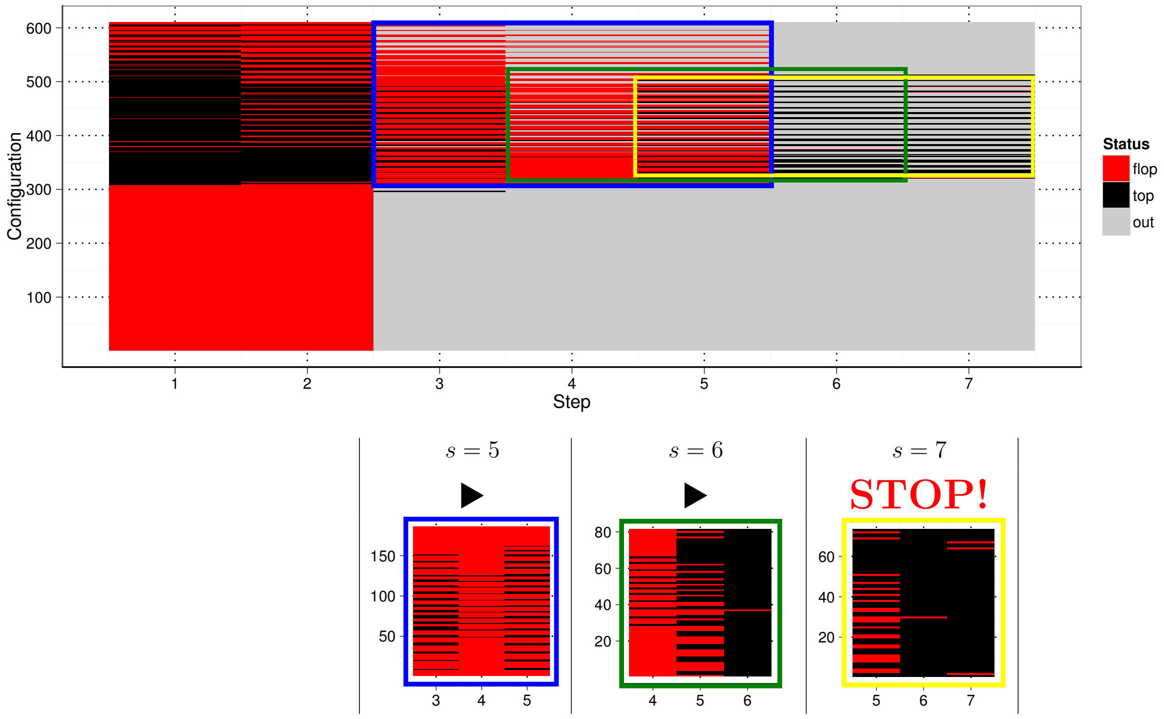

Figure 4: The upper plot shows a run of the CVST algorithm for roughly 600 configurations. At each step a configuration is marked as top (black), flop (red) or dropped (gray). The zoom-ins show the situation for step 5 to 7 without the dropped entries. The early stopping rule takes effect in step 7, because the remaining configurations performed equally well during step 5 to 7.

4.4 Meta-Parameters for the CVST

The CVST algorithm has a number of meta-parameters which the experimenter has to choose beforehand. In this section we give suggestions on how to choose these parameters. The parameter α controls the significance level for the test for similar behavior in each step of the procedure. We suggest to set this to the usual level of $\alpha = 0.05$. Furthermore β_l and α_l control the significance level of the H_0 (configuration is a loser) and H_1 (configuration is a winner) respectively. We suggest an asymmetric setup by setting $\beta_l = 0.1$, since we want to drop loser configurations relatively fast and $\alpha_l = 0.01$, since we want to be really sure when we accept a configuration as overall winner. Finally, we set w_{stop} to 3 for $S = 10$ and 6 for $S = 20$, as we have observed that this choice works well in practice.

5. Properties of the CVST Algorithm

After having introduced the overall concept of the CVST algorithm, we now focus on some properties of the procedure: Exploiting properties of the underlying sequential testing framework, we show how the experimenter can control the algorithm to work in a stable regime. Given some assumptions about the top/flop variables we show that the CVST algorithm performs with high accuracy after a configuration has reached its stable regime. Additionally, we show how the CVST algorithm can be used to work best on a given time budget. Finally, we discuss some unsolved questions and give possible directions for future research.

5.1 Performance in a Stable Regime

As discussed in Section 2 the winning probability of a configuration might change if we feed the learning algorithm more data. Therefore, a reasonable algorithm exploiting the learning on subsets of the data must be capable of dealing with these difficulties and potential change points in the behavior of certain configurations. In this section we investigate some properties of the CVST algorithm which makes it particularly suitable for learning on increasing subsets of the data.

The first property of the open sequential test employed in the CVST algorithm comes in handy to control the overall convergence process and to assure that no configurations are dropped prematurely:

Lemma 1 (Safety Zone) *Given the CVST algorithm with significance level α_l, β_l for being a top or flop configuration respectively, and maximal number of steps S, and a configuration which loses for the first s_{cp} iterations, as long as*

$$0 \leq \frac{s_{cp}}{S} \leq \frac{s_{safe}}{S} \text{ with } s_{safe} = \frac{\log \frac{\beta_l}{1-\alpha_l}}{\log 2 - \sqrt[S]{\frac{1-\beta_l}{\alpha_l}}} \text{ and } S \geq \left\lceil \log \frac{1-\beta_l}{\alpha_l} / \log 2 \right\rceil,$$

the probability that the configuration is dropped prematurely by the CVST algorithm is zero.

Proof The details of the proof are deferred to Appendix D. ■

The consequence of Lemma 1 is that the experimenter can directly control via the significance levels α_l, β_l until which iteration no premature dropping should occur and therefore guide the whole process into a stable regime in which the configurations will see enough data to show their real performance. Note that this property is a direct consequence of the sequential analysis framework and is used here to guide the test into a controlled region where we do not observe a premature dropping of configurations. Equation (2) ensures that we actually perform a meaningful test to discriminate a loser configuration ($\pi_0 = 0.5$) from a winning configuration ($\pi_1 > \pi_0$). Thus, by adjusting the safety zone of the CVST algorithm the experimenter can ensure that the configurations act according to the preconditions of the sequential testing framework introduced in Section 4.2, namely exhibiting a fixed probability π of being a winner configuration at each step.

Note that this safety zone is solely a guard for premature dropping of a configuration due to insufficient data in the first few steps of the CVST algorithm. The experimenter should have a notion at which point the performance of the configurations should stabilize in terms of error behavior, i.e., the learners see enough data to show their real performance. We argue that at this point the configurations behave reasonable stable, thus, fulfilling

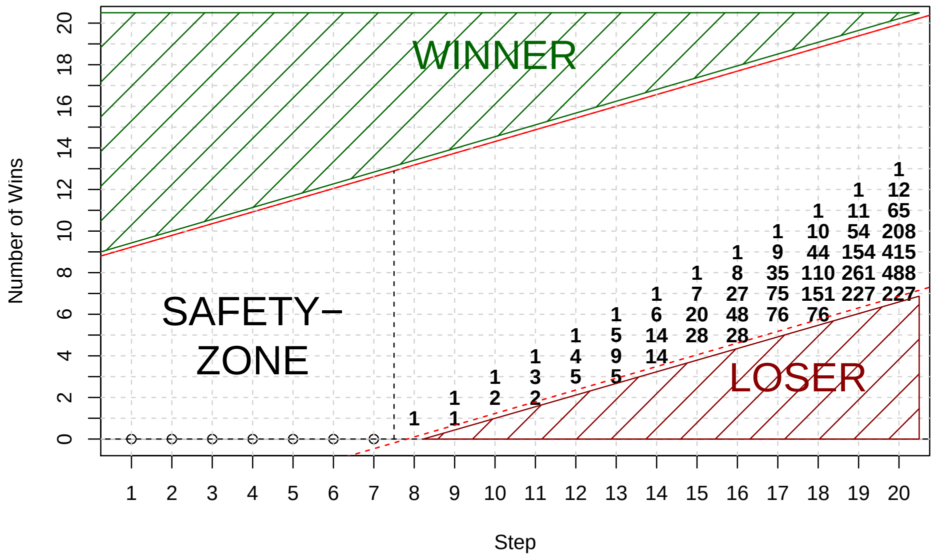

Figure 5: Visualization of the worst-case scenario for the error probability of the CVST algorithm: A global winner configuration is labeled as a constant loser until the safety zone is reached. Then we can calculate the probability that this configuration endures the sequential test by a recurrence scheme, which counts the number of remaining paths ending up in the non-loser region.

both the independence and identically distributed assumption of the sequential learning framework. We are fully aware that these assumptions are strong, yet, backed up by our extensive experimental evaluation in Section 6, we want to shed some light on why the CVST procedure shows such impressive speed-ups with small impact on the accuracy compared to ordinary cross-validation and even outperforms other model selection heuristics.

Hence, we define a *stable* configuration as a configuration which sticks to a certain probability π of being a winning configuration. So after having seen enough data to show its real behavior the robust transformation of the test error of the configuration inside the CVST algorithm (see Section 4.1) exhibits the properties of an i.i.d. Bernoulli variable and thus acts as a *stable* configuration in the subsequent steps of the CVST procedure. So a global winning configuration will be a *stable* configuration with a probability $\pi \gg \pi_0 = 0.5$.

Using these assumptions we can now take a look at the worst case performance of the CVST algorithm. Suppose a global winning configuration has been constantly marked as a loser up to the safety zone, because the amount of data available up to this point was not sufficient to show the superiority of this configuration. Given that the global winning configuration now sees enough data to be marked as a winning configuration by the binarization process throughout the next steps with probability π, we can give an error bound of the overall process by solving specific recurrences.

Figure 5 gives a visual impression of our worst case analysis for the example of a 20 step CVST execution: The winning configuration generated a straight line of zeros up to the safety zone of 7. Our approach to bound the error of the fast cross-validation now consists essentially in calculating the probability mass that ends up in the non-loser region. The following lemma shows how we can express the number of paths which lead to a specific point on the graph by a two-dimensional recurrence relation:

Lemma 2 (Recurrence Relation) *Denote by* $\mathrm{Path}(s_R, s_C)$ *the number of paths, which lead to the point at the intersection of row* s_R *and column* s_C *and lie above the lower decision boundary* L_0 *of the sequential test. Given the worst case scenario described above the number of paths can be calculated as follows:*

$$\mathrm{Path}(s_R, s_C) = \begin{cases} 1 & \textit{if } s_R = 0 \wedge c \leq s_{safe} = \frac{\log \frac{\beta_l}{1-\alpha_l}}{\log 2 - \sqrt[S]{\frac{1-\beta_l}{\alpha_l}}} \\ 1 & \textit{if } s_R = s_C - s_{safe} \\ \mathrm{Path}(s_R, s_C - 1) + \mathrm{Path}(s_R - 1, s_C - 1) & \textit{if } L_0(c) < s_R < s_C - s_{safe} \\ 0 & \textit{otherwise.} \end{cases}$$

Proof We split the proof into the four cases:

1. The first case is by definition: The configuration has a straight line of zeros up to the safety zone s_{safe}.
2. The second case describes the diagonal path starting from the point $(1, s_{\text{safe}} + 1)$: By construction of the paths (1 means diagonal up; 0 means one step to the right) the diagonal path can just be reached by a single combination, namely a straight line of ones.
3. The third case is the actual recurrence: If the given point is above the lower decision bound L_0, then the number of paths leading to this point is equal to the number of paths that lie directly to the left of this point plus the paths which lie directly diagonal downwards from this point. From the first paths this point can be reached by a direct step to the right and from the latter the current point can be reached by a diagonal step upwards. Since there are no other options than that by construction, this equality holds.
4. The last case describes all other paths, which either lie below the lower decision bound and therefore end up in the loser region or are above the diagonal and thus can never be reached.

■

This recurrence is visualized in Figure 5. Each number on the grid gives the number of valid, non-loser paths, which can reach the specific point. With this recurrence we are now able to prove a global, worst-case error probability of the fast cross-validation.

Theorem 3 (Error Bound of CVST for Stable Configuration) *Suppose a global winning configuration has reached the safety zone with a constant loser trace and then switches*

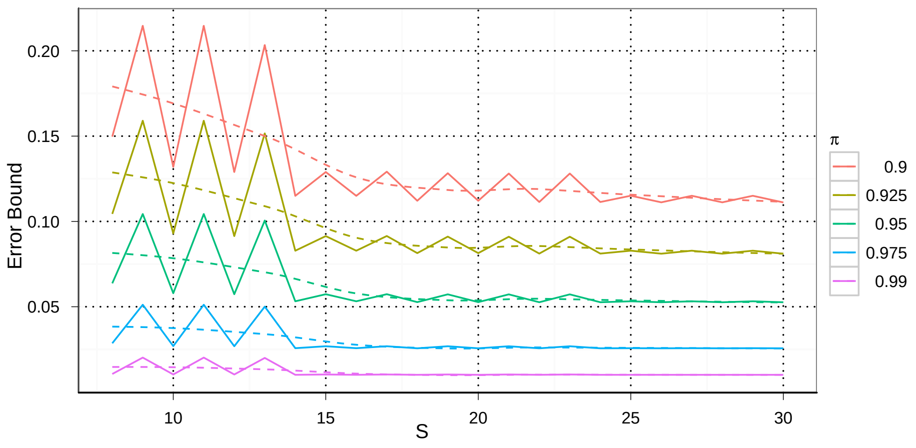

Figure 6: Error bound of the fast cross-validation as proven in Theorem 3 for different success probabilities π and maximal step sizes S. To mark the global trend we fitted a LOESS curve given as dotted line to the data.

to a stable winner configuration with a success probability of $\pi \gg \pi_0 = 0.5$. *Then the error that the CVST algorithm erroneously drops this configuration can be determined as follows:*

$$P(\textit{reject } \pi) \le 1 - \sum_{i=\lfloor L_0(S)\rfloor+1}^{r} \mathrm{Path}(i,S)\pi^i(1-\pi)^{r-i} \qquad \textit{with } r = S - \left\lfloor \frac{\log \frac{\beta_l}{1-\alpha_l}}{\log 2 - \sqrt[S]{\frac{1-\beta_l}{\alpha_l}}} \right\rfloor .$$

Proof The basic idea is to use the number of paths leading to the non-loser region to calculate the probability that the configuration actually survives. This corresponds to the last column of the example in Figure 5. Since we model the outcome of the binarization process as a binomial variable with the success probability of π, the first diagonal path has a probability of π^r. The next paths each have a probability of $\pi^{(r-1)}(1-\pi)^1$ and so on until the last viable paths are reached in the point $(\lfloor L_0(S)\rfloor + 1, S)$. So the complete probability of the survival of the configuration is summed up with the corresponding number of paths from Lemma 2. Since we are interested in the complementary event, we subtract the resulting sum from one, which concludes the proof. ■

Note that the early stopping rule does not interfere with this bound: The worst case is indeed that the process goes on for the maximal number of steps S, since then the probability mass will be maximally spread due to the linear lower decision boundary and the corresponding exponents are maximal. So if the early stopping rule terminates the process before reaching the maximum number of steps, the resulting error probability will be lower than our given bound.

The error bound for different success probabilities and the proposed sequential test with $\alpha_l = 0.01$ and $\beta_l = 0.1$ are depicted in Figure 6. First of all we can observe a relatively fast convergence of the overall error with increasing maximal number of steps S. The impact on

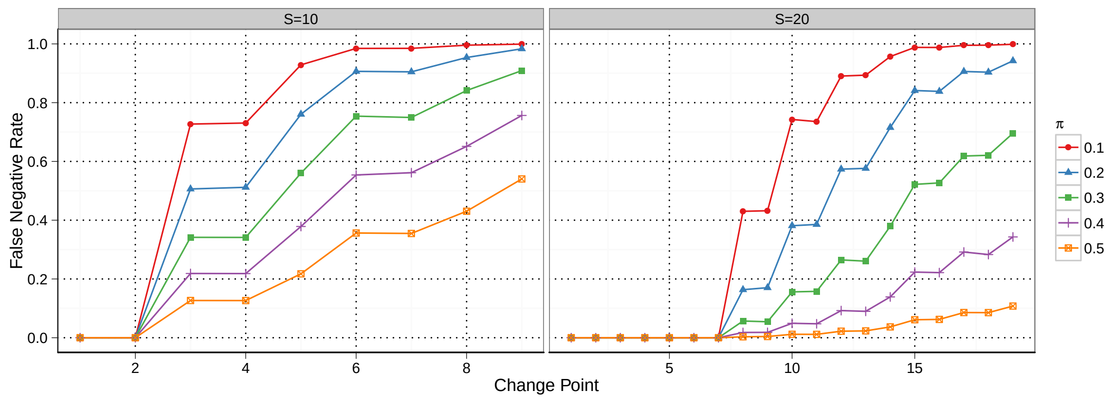

Figure 7: False negatives generated with the open sequential test for non-stationary configurations , i.e., at the given change point the Bernoulli variable changes its π_{before} from the indicated value to 1.0.

the error is marginal for the shown success probabilities, i.e., for instance for $\pi = 0.95$ the error nearly converges to the optimum of 0.05. Note that the oscillations especially for small step sizes originate from the rectangular grid imposed by the interplay of the Path-operator and the lower decision boundary L_0 leading to some fluctuations. Overall, the chosen test scheme allows us not only to control the safety zone but also has only a small impact on the error probability, which once again shows the practicality of the open sequential ratio test for the fast cross-validation procedure. By using this statistical test we can balance the need for a conservative retention of configurations as long as possible with the statistically controlled dropping of significant loser configurations with nearly no impact on the overall error probability.

Our analysis assumes that the experimenter has chosen the right safety zone for the learning problem at hand. For small data sizes it could happen that this safety zone was chosen too small, therefore the change point of the global winning configuration might lie outside the safety zone. While this will not occur often for today's sizes of data sets we have analyzed the behavior of CVST under this circumstances to give a complete view of the properties of the algorithm. To get insight into the drop rate for the case when the experimenter underestimated the change point s_{cp} we simulate those switching configurations by independent Bernoulli variables which change their success probability π from a chosen $\pi_{\text{before}} \in \{0.1, 0.2, \dots, 0.5\}$ to a constant 1.0 at a given change point. This behavior essentially imitates the behavior of a switching configuration which starts out as a loser (i.e., up to the change point the trace will consist more or less of zeros) and after enough data is available turns into a constant winner.

The relative loss of these configurations for 10 and 20 steps is plotted in Figure 7 for different change points. The figure reveals our theoretical findings of Lemma 1 showing the corresponding *safety zone* for the specific parameter settings: For instance for $\alpha_l =$ 0.01 and $\beta_l = 0.1$ and $S = 10$ steps, the safety zone amounts to 0.27×10, meaning that

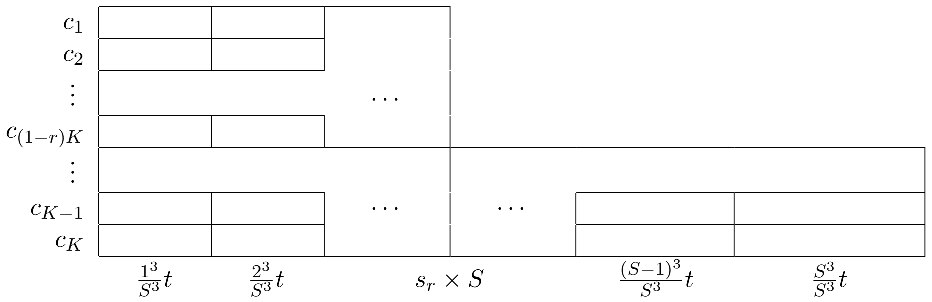

Figure 8: Approximation of the time consumption for a cubic learner. In each step we calculate a model on a subset of the data, so the model calculation time t on the full data set is adjusted accordingly. After $s_r \times S$ steps of the process, we assume a drop to $r \times K$ remaining configurations.

if the change point for all switching configurations occurs at step one or two, the CVST algorithm would not suffer from false positives. Similarly, for $S = 20$ the safety zone is $0.39 \times 20 = 7.8$. These theoretical results are confirmed in our simulation study, where the false negative rate is zero for sufficiently small change points for the open variant of the test. After that, there are increasing probabilities that the configuration will be removed. Depending on the success probability of the configuration before the change point, the resulting false negative rate ranges from mild for $\pi = 0.5$ to relatively severe for $\pi = 0.1$. The later the change point occurs, the higher the resulting false negative rate will be. Interestingly, if we increase the total number of steps from 10 to 20, the absolute values of the false negative rates are significantly lower. So even when the experimenter underestimates the actual change point, the CVST algorithm has some extra room which can even be extended by increasing the total number of steps.

5.2 Fast-Cross Validation on a Time Budget

While the CVST algorithm can be used out of the box to speed up regular cross-validation, the aforementioned properties of the procedure come in handy when we face a situation in which an optimal parameter configuration has to be found given a fixed computational budget. If the time is not sufficient to perform a full cross-validation or the amount of data that has to be processed is too big to explore a sufficiently spaced parameter grid with ordinary cross-validation in a reasonable time, the CVST algorithm can easily be adjusted to the specified time constraint. Thus, the experimenter is able to get the maximal number of model evaluations given the time budget available to judge which model is the best.

This is achieved by calculating a maximal steps parameter S which leads to a near coverage of the available time budget T as depicted in Figure 8. The idea is to specify an expected drop rate $(1 - r)$ of configurations and a safety zone bound s_{safe}. Then we can give a rough estimate of the total time needed for a CVST with a total number of steps S, equating this with the available time budget T and solving for S. More formally, given K parameter configurations and a pre-specified safety zone bound $s_{\text{safe}} = s_r \times S$ with

$0 < s_r < 1$ to ensure that no configuration is dropped prematurely, the computational demands of the CVST algorithm are approximated by the sum of the time needed before step s_{safe} involving the model calculation of all K configurations and after step s_{safe} for $r \times K$ configurations with $0 < r < 1$. As we will see in the experimental evaluation section, this assumption of a given drop rate of $(1 - r)$ leading to the form of time consumption as depicted in Figure 8 is quite common. The observed drop rate corresponds to the overall difficulty of the problem at hand.

Given the computation time t needed to perform the model calculation on the full data set, we prove in Appendix E that the optimal maximum step parameter for a learner of time complexity $f(n) = n^m$ can be calculated as follows:

$$S = \Bigg\lfloor \frac{m+1}{4}\frac{2T - tK(1-r)s_r^m + tKr}{((1-r)s_r^{m+1}+r)tK} + \sqrt{\left[\frac{m+1}{4}\frac{2T - tK(1-r)s_r^m + tKr}{((1-r)s_r^{m+1}+r)tK}\right]^2 - \frac{m(m+1)}{12}\frac{(1-r)s_r^{m-1}+r}{(1-r)s_r^{m+1}+r}} \Bigg\rfloor .$$

After calculating the maximal number of steps S given the time budget T, we can use the results of Lemma 1 to determine the maximal β_l given a fixed α_l, which yields the requested safety zone bound s_{safe}.

5.3 Discussion of Further Theoretical Analyses

In Section 2 we have noted that in order for the test performances to converge, the parameter configurations should be independent of the sample size. As shown in Appendix A this holds for a range of standard methods in machine learning. Yet, special care has to be taken to really ensure this assumption. For instance for kernel ridge regression one has to scale the ridge parameter during each step of the CVST algorithm to accommodate for the change in the learning set size (see the reference implementation in the official CRAN package named `CVST` or the development version at `https://github.com/tammok/CVST`). The ν-Support Vector Machine on the other hand directly incorporates this scaling of parameters which makes it a good fit for the CVST algorithm. Generally, it would be preferable to have this scaling automatically incorporated in the CVST algorithm such that the experimenter could plug-in his favorite method without the need to think about any scaling issues of hyper-parameters. Unfortunately, this is highly algorithm dependent and, thus, is an open problem for further research.

An additional concern to the practitioner is how to choose the correct size of the safety zone s_{safe}. If the training set does not contain enough data to get to a stable regime of the parameter configurations, even regular cross-validation on the full data set would yield incorrect configurations. But if we have just barely enough data to reach this stable region, setting the right safety zone is essential for the CVST algorithm to return the correct configurations. Unfortunately we are not aware of any test or bound which could hint at the right safety zone given a data set and learner. Yet, in today's world of big data where sample sizes are more often too big than too small, this might not pose a serious problem anymore. Nevertheless, we have analyzed the behavior of the CVST algorithm in case the experimenter underestimates the safety zone in Section 5.1 showing that even for these cases CVST is able to absorb a certain amount of misspecification.

The similarity test introduced in Section 4.1 relies on two assumptions: First, the averaged loss function over the data not used for training in one step gives us a good indicator of the performance of a configuration. Second, well performing configurations show similar behavior in classification or regression on the data not used for learning. While these assumptions definitely make sense, they encode a certain optimism of how the grid of configurations is populated: If we have too few configurations as input to the procedure it might happen that some non-optimal configurations mask out the other, normally optimal, configurations just by chance. To overcome this problem we therefore would need a certain amount of redundancy in the configuration grid. Both the amount of redundancy and thus the similarity measure underlying this redundancy assumption are hard to grasp theoretically, yet, it could lead to new ways to model the binary transformation of the performance of configurations in each step of the CVST algorithm.

There might be even further potential in the behavior of similar configurations that could be used in the CVST algorithm: If there is a notion of similarity between different configurations, it would be interesting to exploit this information and incorporate it into the CVST algorithm. For instance, one could add this kind of information in the function topConfigurations of Algorithm 1 to average the result of similar configurations and, hence, extend the pooling effect of the test already available for the data point dimension in the direction of configurations.

While the selection scheme explained in Section 4.2 deals with the fact of potential change points of a configuration, it is not clear how independent the individual entries of a trace for a given configuration are and how much these potential dependencies influence the power of the sequential testing framework. Preliminary experiments comparing the CVST algorithm as described in this paper and a version of the CVST algorithm where at each step the data pool is shuffled, thus, yielding always different data points for learning and evaluation, showed no significant differences between these two versions. This indicates that at least the potential dependencies introduced by the overlap of learning sets due to subsequent addition of data points do not interfere with the dependency assumption of the sequential testing framework. We will see in the evaluation section that the CVST procedure in its current form shows excellent behavior throughout a wide range of data sets; yet, further research of the theoretical properties of CVST might yield even better procedures in the future.

6. Experiments

Before we evaluate the CVST algorithm on real data, we investigate its performance on controlled data sets. Both for regression and classification tasks we introduce special tailored data sets to highlight the overall behavior and to stress-test the fast cross-validation procedure. To evaluate how the choice of learning method influences the performance of the CVST algorithm, we compare kernel logistic regression (KLR) against a ν-Support Vector Machine (SVM) for classification problems and kernel ridge regression (KRR) versus ν-SVR for regression problems each using a Gaussian kernel (see Roth, 2001; Schölkopf et al., 2000). In all experiments we use a 10 step CVST with parameter settings as described in Section 4.4 (i. e. $\alpha = 0.05, \alpha_l = 0.01, \beta_l = 0.1, w_{\text{stop}} = 3$) to give us an upper bound of the expected speed gain. Note that we could get even higher speed gains by either lowering the

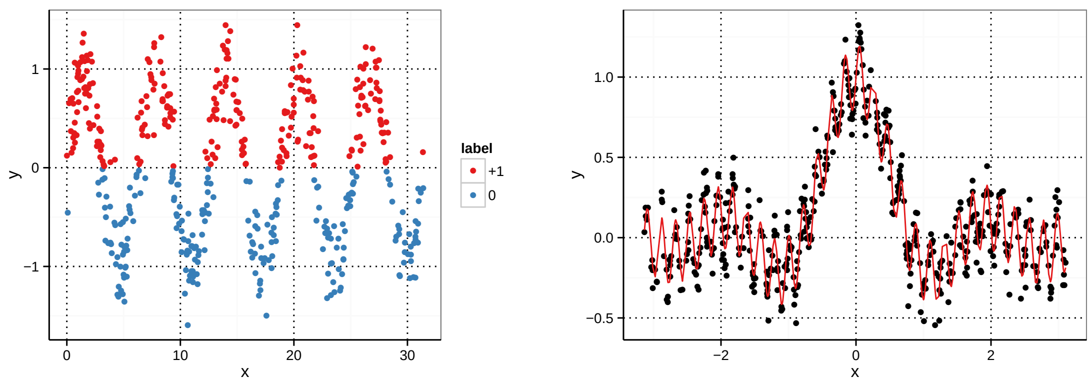

Figure 9: The *noisy sine* (left) and *noisy sinc* data set (right).

number of steps or increasing β_l. From a practical point of view we believe that the settings studied are highly realistic.

6.1 Artificial Data Sets

To assess the quality of the CVST algorithm we first examine its behavior in a controlled setting. We have seen in our motivation section that a specific learning problem might have several layers of structure which can only be revealed by the learner if enough data is available. For instance in Figure 2(a) we can see that the first optimal plateau occurs at $\sigma = 0.1$, while the real optimal parameter centers around $\sigma = 0.01$. Thus, the real optimal choice just becomes apparent if we have seen more than 200 data points.

In this section we construct a learning problem both for regression and classification tasks which could pose severe problems for the CVST algorithm: If it stops too early, it will return a suboptimal parameter set. We evaluate how different intrinsic dimensionalities of the data and various noise levels affect the performance of the procedure. For classification tasks we use the *noisy sine* data set, which consists of a sine uniformly sampled from a range controlled by the intrinsic dimensionality d:

$$y = \sin(x) + \epsilon \quad \text{with } \epsilon \sim \mathcal{N}(0, n^2), x \in [0, 2\pi d], n \in \{0.25, 0.5\}, d \in \{5, 50, 100\}.$$

The labels of the sampled points are just the sign of y. An example for $d = 5, n = 0.25$ is plotted in the left subplot of Figure 9. For regression tasks we devise the *noisy sinc* data set, which consists of a sinc function overlayed with a high-frequency sine:

$$y = \operatorname{sinc}(4x) + \frac{\sin(15dx)}{5} + \epsilon \text{ with } \epsilon \sim \mathcal{N}(0, n^2), x \in [-\pi, \pi], n \in \{0.1, 0.2\}, d \in \{2, 3, 4\}.$$

An example for $d = 2, n = 0.1$ is plotted in the right subplot of Figure 9. For each of these data sets we generate 1,000 data points and run a 10 step CVST and compare its results with a normal 10-fold cross-validation on the full data set. We record both the test error on additional 10,000 data points and the time consumed for the parameter search. The explored parameter grid contains 610 equally spaced parameter configurations

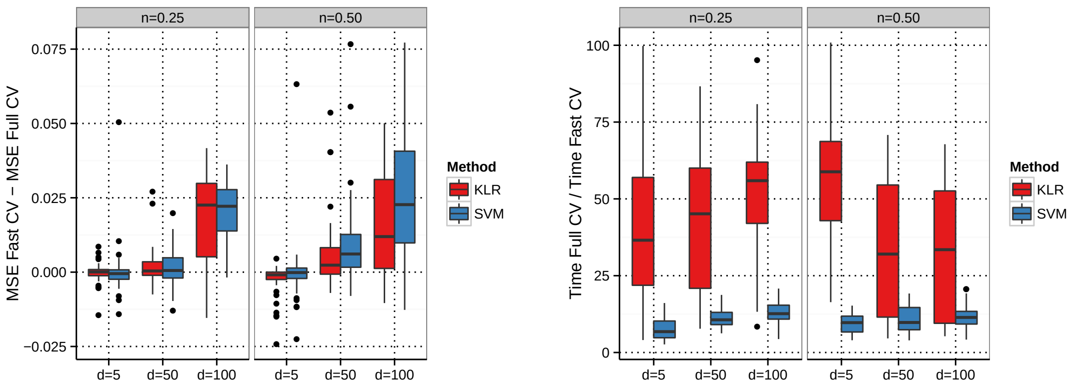

Figure 10: Difference in mean square error (left) and relative speed gain (right) for the *noisy sine* data set.

for each method ($\log_{10}(\sigma) \in \{-3, -2.9, \ldots, 3\}$ and $\nu \in \{0.05, 0.1, \ldots, 0.5\}$ for SVM/SVR and $\log_{10}(\lambda) \in \{-7, -6, \ldots 2\}$ for KLR/KRR, respectively). This process is repeated 50 times to gather sufficient data for an interpretation of the overall process. Apart from recording the difference in mean square error (MSE) of the learner selected by normal cross-validation and by the CVST algorithm we also look at the relative speed gain. Note that we have encoded the classes as 0 and 1 for the classification experiments so the MSE corresponds to the misclassification rate of the learner. So the difference in MSE gives us a good measurement of the impact of using the CVST algorithm for both classification and regression experiments.

The results for the *noisy sine* data set can be seen in Figure 10. The left boxplots show the distribution of the difference in MSE of the best parameter determined by CVST and normal cross-validation. In the low noise setting ($n = 0.25$) the CVST algorithm finds the same optimal parameter as the normal cross-validation up to the intrinsic dimensionality of $d = 50$. For $d = 100$ the CVST algorithm gets stuck in a suboptimal parameter configuration yielding an increased classification error compared to the normal cross-validation. This tendency is slightly increased in the high noise setting ($n = 0.5$) yielding a broader distribution. The classification method used seems to have no direct influence on the difference, both SVM and KLR show nearly similar behavior. This picture changes when we look at the speed gains: While the SVM nearly always ranges between 10 and 20, the KLR shows a speed-up between 20 and 70 times. The variance of the speed gain is generally higher compared to the SVM which seems to be a direct consequence of the inner workings of KLR: The main loop performs at each step a matrix inversion of the whole kernel matrix until the calculated coefficients converge. Obviously this convergence criterion leads to a relative wide-spread distribution of the speed gain when compared to the SVM performance.

Figure 11 shows the distribution of the number of remaining configurations after each step of the CVST algorithm. In the low noise setting (upper row) we can observe a tendency of higher drop rates up to $d = 100$. For the high noise setting (lower row) we observe a

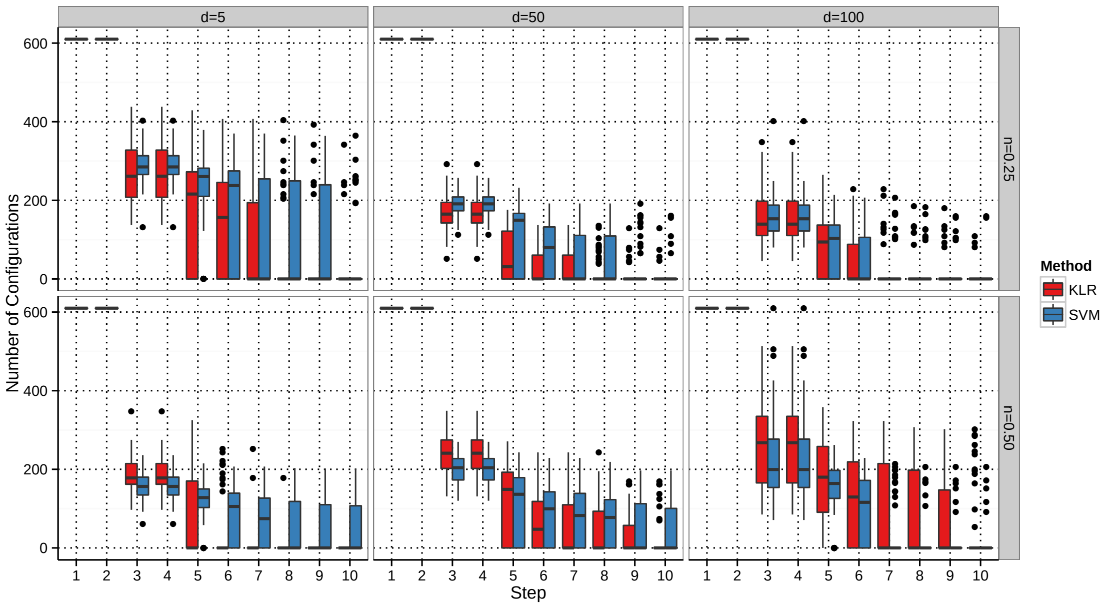

Figure 11: Remaining configurations after each step for the *noisy sine* data set.

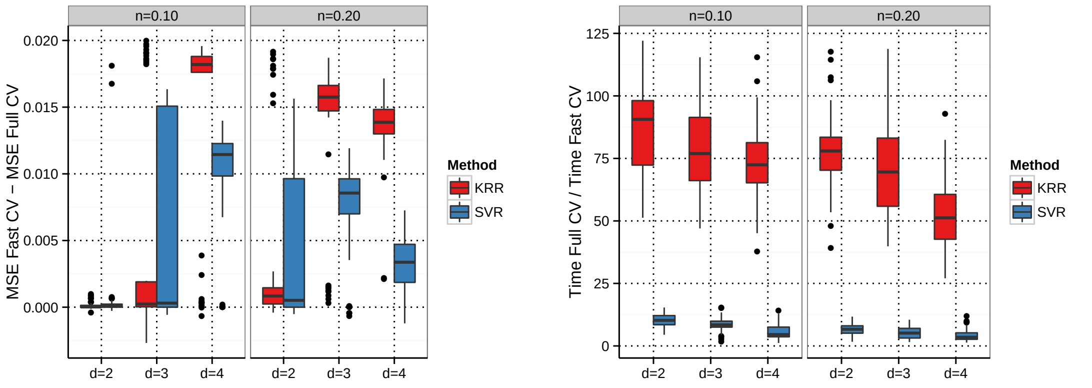

Figure 12: Difference in mean square error (left plots) and relative speed gain (right plots) for the *noisy sinc* data set.

steady increase of kept configurations combined with a higher spread of the distribution. Overall we see a very effective drop rate of configurations for all settings. The SVM and the KLR show nearly similar behavior so that the higher speed gain of the KLR we have seen before is a consequence of the algorithm itself and is not influenced by the CVST algorithm.

The performance on the *noisy sinc* data set is shown in Figure 12. The first striking observation is the transition of the CVST algorithm which can be observed for the intrinsic

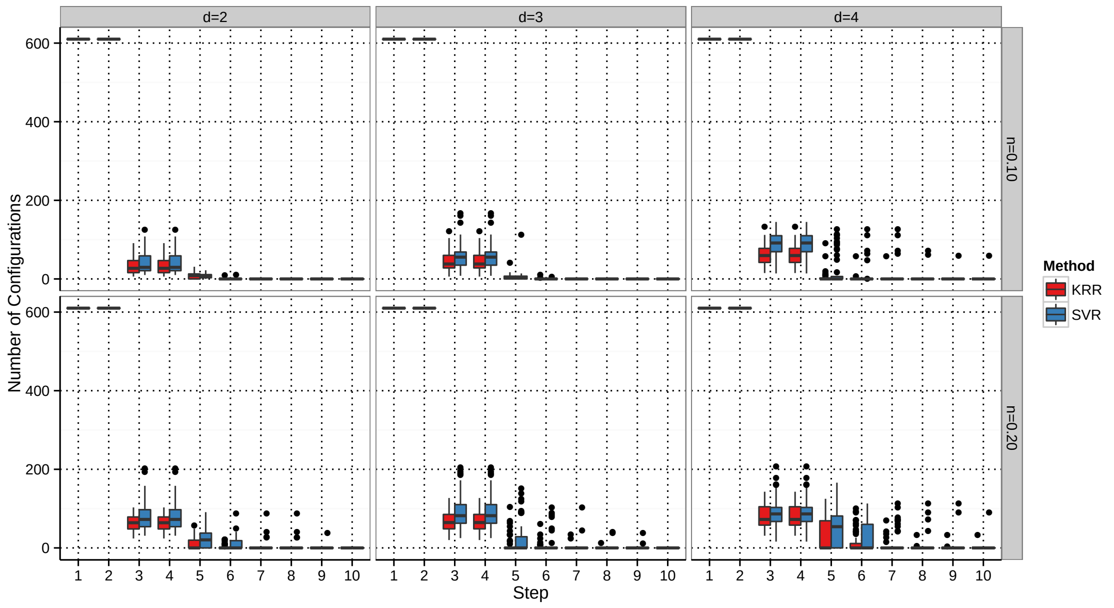

Figure 13: Remaining configurations after each step for the *noisy sinc* data set.

dimensionality of $d = 3$. At this point the overall excellent performance of the CVST algorithm is on the verge of choosing a suboptimal parameter configuration. This behavior is more evident in the high noise setting. In the case of SVR the difference to the solution found by the normal cross-validation is always smaller than for KRR. The speed gain observed shows a small decline over the different dimensionalities and noise levels and ranges between 10 and 20 for the SVR and 50 to 100 for KRR.

This is a direct consequence of the behavior which can be observed in the number of remaining configurations shown in Figure 13. Compared to the classification experiments the drop is much more drastic. The intrinsic dimensionality and the noise level show a small influence (higher dimensionality or noise level yields more remaining configurations) but the overall variance of the distribution is much smaller than in the classification experiments.

In Figure 14 we examine the influence of more data on the performance of the CVST algorithm. Both for the *noisy sine* and *noisy sinc* data set we are able to estimate the correct parameter configuration for all noise and dimensionality settings if we feed the CVST with enough data.[1] Clearly, the CVST is capable of extracting the right parameter configuration if we increase the amount of data to 2000 or 5000 data points, rendering our method even more suitable for big data scenarios: If data is abundant, CVST will be able to estimate the correct parameter in a much smaller time frame.

1. Note that we have to limit this experiment to the SVM/SVR method, since the full cross-validation of the KLR/KRR would have taken too much time to compute.

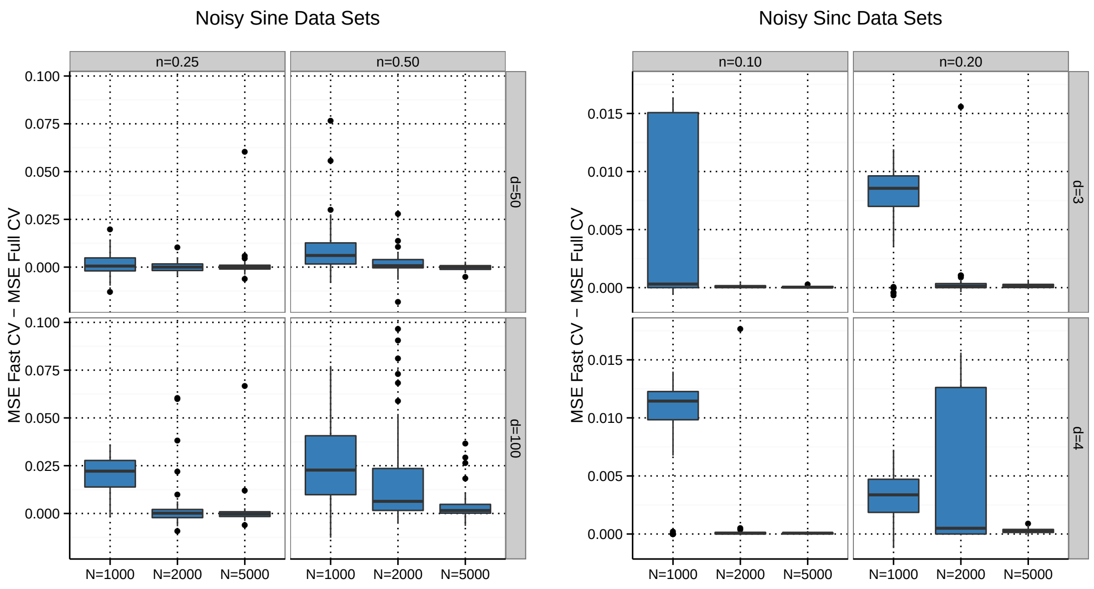

Figure 14: Difference in mean square error for SVM/SVR with increasing data set size for *noisy sine* (left) and the *noisy sinc* (right) data sets. By adding more data, the CVST algorithm converges to the correct parameter configuration.

6.2 Benchmark Data Sets

After demonstrating the overall performance of the CVST algorithm on controlled data sets we will investigate its performance on real life and well known benchmark data sets. For classification we picked a representative choice of data sets from the IDA benchmark repository (see Rätsch et al. 2001[2]). Furthermore we added the first two classes with the most entries of the *covertype* data set (see Blackard and Dean, 1999). Then we follow the procedure of the paper in sampling 2,000 data points of each class for the model learning and estimate the test error on the remaining data points. For regression we pick the data used in Donoho and Johnstone (1994) and add the *bank32nm*, *pumadyn32nm* and *kin32nm* of the Delve repository.[3]

We process each data set as follows: First we normalize each variable of the data to zero mean and variance of one, and in case of regression we also normalize the dependent variable. Then we split the data set in half and use one part for training and the other for the estimation of the test error. This process is repeated 50 times to get sufficient statistics for the performance of the methods. As in the artificial data setting we compare the speed gain of the fast compared to the normal cross-validation on the same parameter grid of 610 values. To allow for better comparability of the performance on the different data sets we report the mean square error (MSE) ratio of the CVST procedure compared to the normal

2. Available at `http://www.mldata.org`.
3. Available at `http://www.cs.toronto.edu/~delve`.

Data	Method	MSE Ratio	Speed	Data	Method	MSE Ratio	Speed
banana	KLR	$\mathbf{0.998 \pm 0.012}$	61.1	bank	KRR	0.994 ± 0.003	85.7
banana	SVM	$\mathbf{1.001 \pm 0.008}$	16.9	bank	SVR	0.998 ± 0.001	43.9
covtype	KLR	$\mathbf{0.994 \pm 0.011}$	84.3	blocks	KRR	0.762 ± 0.022	81.3
covtype	SVM	0.939 ± 0.009	53.4	blocks	SVR	0.886 ± 0.016	39.5
german	KLR	$\mathbf{0.987 \pm 0.017}$	27.5	bumps	KRR	0.784 ± 0.043	86.1
german	SVM	$\mathbf{0.981 \pm 0.024}$	5.5	bumps	SVR	0.666 ± 0.030	37.3
image	KLR	$\mathbf{1.032 \pm 0.051}$	33.5	doppler	KRR	0.766 ± 0.035	92.4
image	SVM	0.923 ± 0.060	13.8	doppler	SVR	0.937 ± 0.014	41.2
ringnorm	KLR	0.814 ± 0.050	111.7	heavisine	KRR	0.981 ± 0.005	53.2
ringnorm	SVM	$\mathbf{0.999 \pm 0.017}$	32.4	heavisine	SVR	0.988 ± 0.003	33.7
splice	KLR	$\mathbf{0.991 \pm 0.019}$	52.2	kin	KRR	0.994 ± 0.002	58.7
splice	SVM	$\mathbf{1.005 \pm 0.016}$	18.1	kin	SVR	0.996 ± 0.001	39.9
twonorm	KLR	$\mathbf{1.017 \pm 0.034}$	50.1	pumadyn	KRR	0.992 ± 0.003	68.2
twonorm	SVM	$\mathbf{1.015 \pm 0.014}$	25.7	pumadyn	SVR	0.984 ± 0.007	29.6
waveform	KLR	$\mathbf{0.989 \pm 0.014}$	54.0				
waveform	SVM	$\mathbf{0.992 \pm 0.013}$	22.8				

Table 2: Comparison of performance of the CVST algorithm to full cross-validation (classification data sets in left part, regression data sets in right part). MSE ratio is the relative gain in MSE of CVST compared to the full cross-validation. Speed denotes the relative speed increase of CVST compared to the full cross-validation. We report the mean values over 50 repetitions and 1.96 standard errors. If CVST performs on par or better than the full cross-validation (i.e., MSE ratio plus 1.96 standard errors is bigger than 1.0) the values are in boldface.

cross-validation, i.e., values over 1.0 favor the CVST procedure. For the *blocks*, *bumps*, and *doppler* data set of Donoho and Johnstone (1994) we adjusted the range of σ to a smaller scale ($\log_{10}(\sigma) \in \{-6, -5.9, \ldots, 0\}$) to have reasonable results in the parameter grid of 610 values since these data sets contain a very fine-grained structure. Note that this adjustment is just for the sake of comparability to the other data sets.

Figure 15 shows the result for the classification data sets (left side) and the regression data sets (right side). The upper panels depict the relative gain in MSE of CVST compared to the full cross-validation. For the classification tasks we see that CVST is on par with the full cross-validation except for the SVM for *covtype* and KLR for *ringnorm*. For the regression task we observe that except for the *blocks*, *bumps* and *doppler* data sets CVST chooses reasonable parameter set. Although for some problems the CVST algorithm picks a suboptimal parameter set, even then the relative performance decreases are always relatively small and range around 80%. The learners have hardly any impact on the behavior; just for the *ringnorm* and the *blocks*, *bumps* and *doppler* data set we see a strong difference of the corresponding methods. These findings can also be observed in Table 2: Given the mean of the relative MSE ratio and the speed ratio with its corresponding 1.96 standard errors we mark entries in boldface where the MSE ratio plus the 1.96 standard error is bigger than 1.0 indicating a performance on par or better than the normal cross-validation. While CVST can tackle most of the classification task we see a relative decline in the regression tasks.

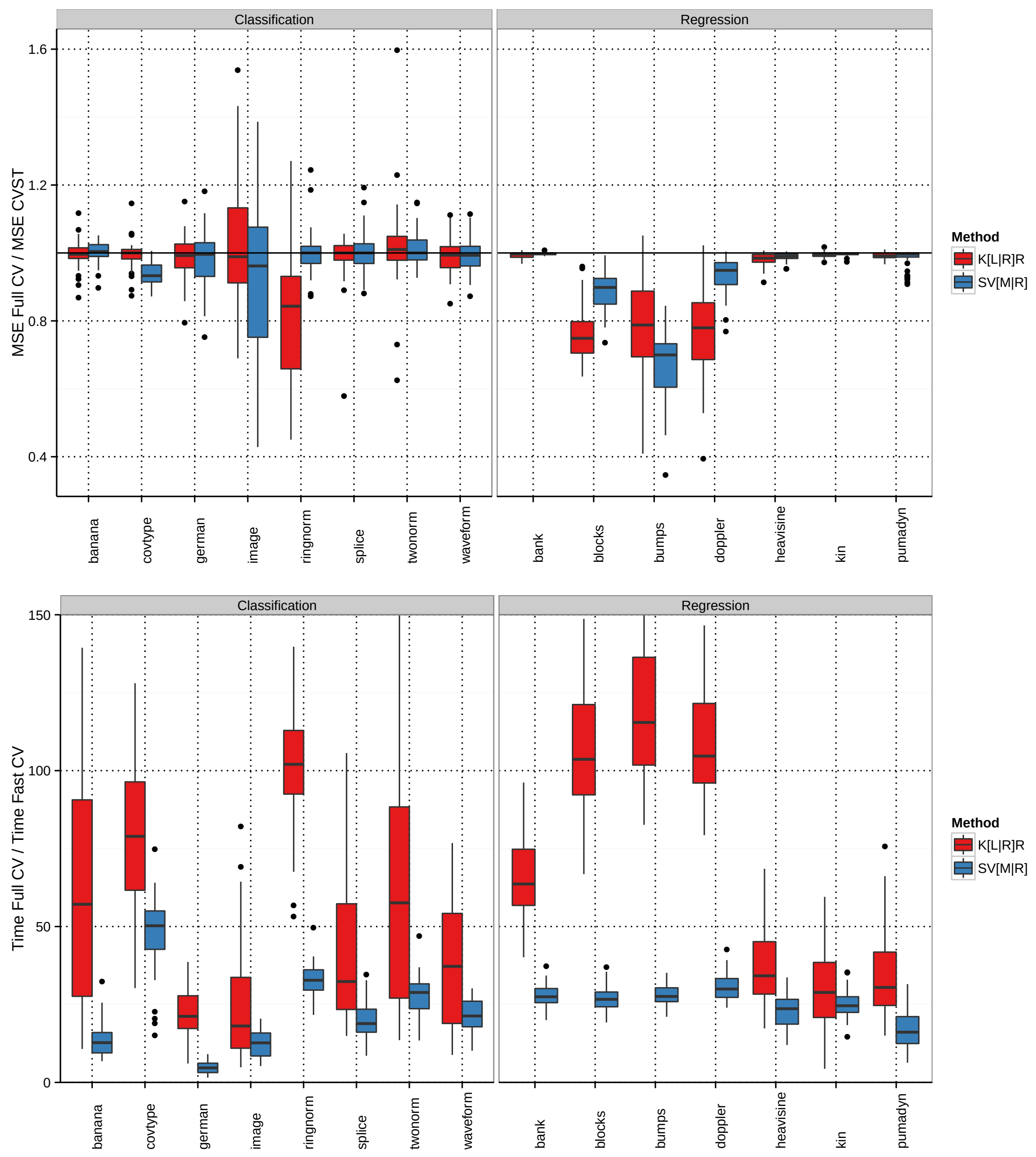

Figure 15: MSE ratio (upper plots) and relative speed gain (lower plots) for the *benchmark* data sets.

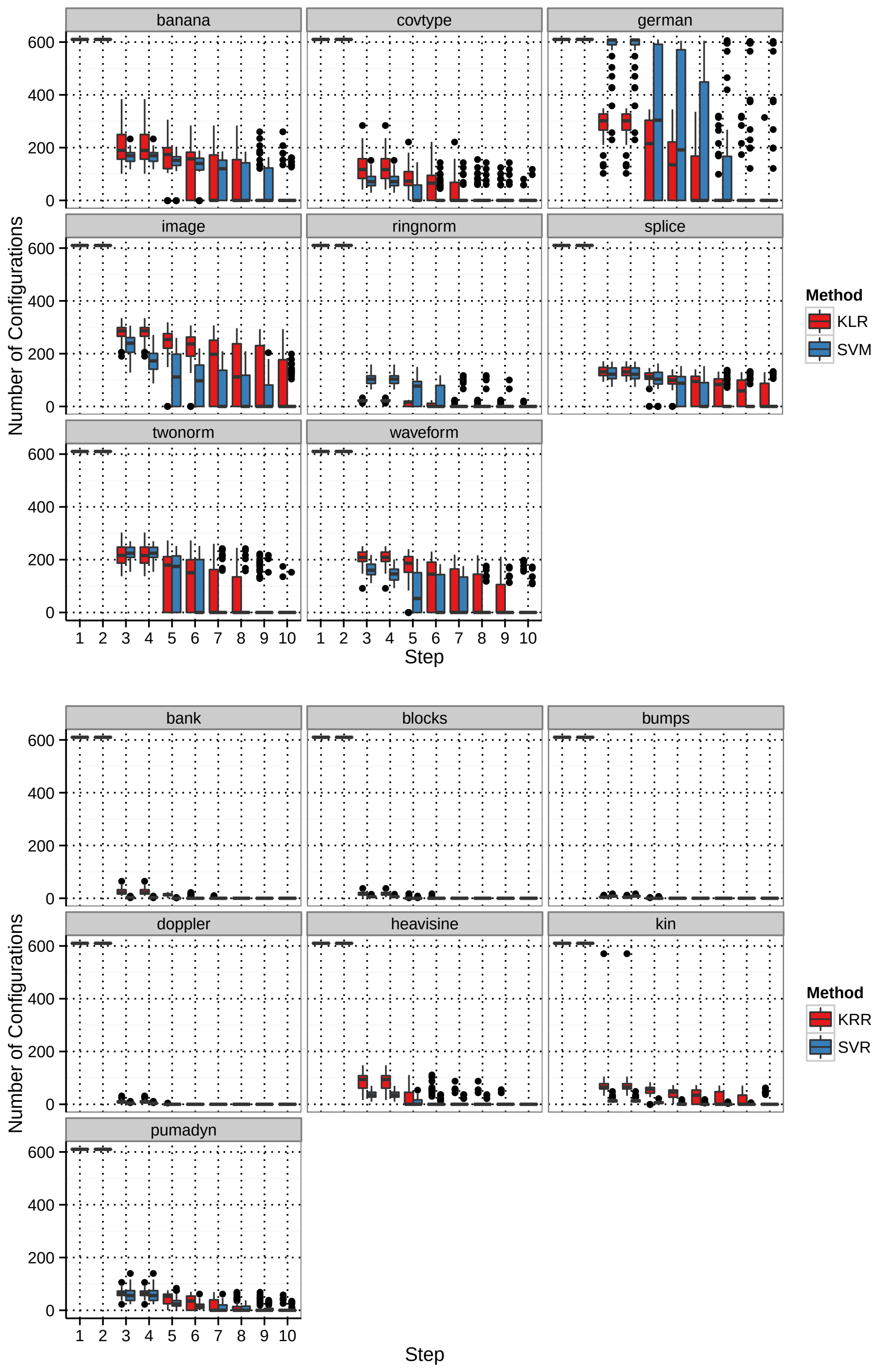

Figure 16: Remaining configurations after each step for different *benchmark* data sets.

But except for the *blocks*, *bumps* and *doppler* data sets the relative performance decrease ranges around 99% indicating a nearly optimal performance.

In terms of speed gain we see a much more diverse and varying picture. Overall, the speed improvements for KLR and KRR are higher than for SVM and SVR and reach up to 120 times compared to normal cross-validation. Regression tasks in general seem to be solved faster than classification tasks, which can clearly be explained when we look at the traces in Figure 16: For classification tasks the number of kept configurations is generally much higher than for the regression tasks. Furthermore we can observe several types of difficulty of the learning problems. For instance the *german* data set seems to be much more difficult than the *ringnorm* data (see Braun et al., 2008) which is also reflected in the difference and speed improvement seen in the previous figure. We will see in Section 7.1 that we can trade time for increasing the accuracy of CVST for the regression tasks by leveraging the modular construction of the CVST procedure.

Since finding the top configurations inside the loop of the CVST algorithm is a crucial step to the overall performance of the procedure we further investigate how our choice of tests influence the performance of the CVST procedure. Recall from Algorithm 2 that we used the Cochran's Q test for classification experiments (see line 9) and Friedman test for regression problems (see line 11) to find the top configurations in an iterative testing scheme. Both these test are non-parametric and paired tests, i.e., they both take into account the pointwise performance of a configuration and, thus, compare the performance on individual data points. In Section 4.1 we argued that this pooling effect robustifies the estimation of the top configurations since outliers in the testing data do not have such a dramatic effect on the test results compared to using for instance the overall test error as input for the test. To verify this claim we have replaced the tests in the Algorithm 2 by unpaired, non-parametric versions which solely test whether the test error is significantly different without taking the results of the individual data points into account. To this end we have replaced the Cochran's Q test for classification experiments on line 9 of Algorithm 2 by an unpaired version described by Wilson (1927) and the Friedman test by the Kruskal-Wallis rank sum test (Kruskal and Wallis, 1952). Again we repeat the procedure for each benchmark set 50 times to get reliable statistics.

The results are reported in Table 3, upper part. We can see that the relative level of MSE is almost always around 1.0 if we take the 1.96 standard error ranges into account. The upper plot of Figure 17 shows the distribution of the MSE ratio. Except for the *bumps* and *doppler* data set all distributions are clearly centered around 1.0 with a narrow spread which further highlights the equality of the two methods in terms of accuracy.

Comparing the ratio of the CVST procedure to the unpaired variant we can see that the paired test variant improves the runtime of the procedure significantly. This clearly demonstrates that the usage of the paired tests which directly estimate the top configurations on the pointwise predictions saves computation time with no impact on the accuracy.

Since we compared the CVST algorithm to a full cross-validation it is also of interest to see how CVST compares to a simple heuristic which uses just 10% of the data for the cross-validation. We have executed this experiment for all benchmark data sets and repeated the procedure 50 times to get statistically sound estimates. The middle part of Table 3 reports the MSE ratio of the CVST compared to the 10% cross-validation annotated with their corresponding 1.96 standard errors and again the speed ratio. The first striking thing to observe is that the MSE ratios are all significantly bigger than 1.0, indicating that CVST always finds a better performing configuration than the simple 10% heuristic. While the accuracy impact varies across the different data sets CVST always picks significantly better performing configurations with a modest impact on the runtime compared to the simple 10% heuristic. This trend can clearly be seen in the middle plot of Figure 17 which shows the corresponding distributions of the relative level of MSE. For all data sets the bulk of the distribution is above 1.0 indicating better performance of the CVST method compared to the 10% heuristic.

The last comparison of the performance of the CVST method is shown in the lower part of Table 3. Here we show the MSE ratio of CVST compared to a random search as described in Bergstra and Bengio (2012). In each step of the random search procedure we choose parameters uniformly distributed over the range of the corresponding grid of the CVST procedure and learn a full-data model. After having spent the same amount of time as the CVST procedure on a specific data set we stop the random search. Then we pick the best model of the so far evaluated parameters and compare its performance to the CVST model. Again, the lower part of Table 3 shows the relative gain in MSE and their corresponding 1.96 standard errors gathered over 50 repetitions for each data set. Both the table and the lower part of Figure 17 indicate that CVST shows better performance compared to random search especially in the regression data sets. In some cases (*covtype* with SVM, *ringnorm* with SVM and *splice* with SVM) the random search outperforms CVST but in the majority of cases the CVST procedure can extract better parameter configurations in the same amount of time than the random search.

In summary, the evaluation of the benchmark data sets shows that the CVST algorithm gives a huge speed improvement compared to the normal cross-validation. While we see some non-optimal choices of configurations, the total impact on the error is never exceptionally high. We have to keep in mind that we have chosen the parameters of our CVST algorithm to give an impression of the maximal attainable speed-up: More conservative settings would trade computational time for lowering the impact on the test error. The CVST outperforms both unpaired variants of the procedure, the simple heuristics of cross-validation on just 10% of the data, and a random search in parameter space. This clearly demonstrates that the individual parts of the CVST procedure are well chosen and the combination of tests are superior to other methods. Trading some speed compared to simpler heuristics for more robust and stable estimates of optimal performing configurations and the huge speed improvement compared to a full cross-validation renders the CVST procedure as a promising candidate for model selection in big data settings.

7. Modularization and Extensions

In this Section we will deal with several aspects of the CVST algorithm: We illuminate the inner structure of the overall procedure and discuss potential extensions and properties of specific steps. The CVST algorithm consists of a sequence of tightly coupled modules: The output of the top or flop test is the input for the subsequent test for significant losers. The performance history of all remaining configurations is then the input for the early stopping rule which looks for similar performance of the remaining configurations on the learning problem to capture the right point in time to stop the CVST loop. This stepwise procedure

Data	Method	MSE Ratio	Speed	Data	Method	MSE Ratio	Speed
banana	KLR	1.001 ± 0.010	2.9	bank	KRR	0.984 ± 0.005	3.0
banana	SVM	1.005 ± 0.009	1.6	bank	SVR	1.000 ± 0.001	1.2
covtype	KLR	1.003 ± 0.005	1.6	blocks	KRR	0.957 ± 0.030	1.4
covtype	SVM	0.992 ± 0.007	1.2	blocks	SVR	0.986 ± 0.006	1.4
german	KLR	0.993 ± 0.013	0.9	bumps	KRR	0.920 ± 0.074	1.0
german	SVM	0.984 ± 0.019	0.6	bumps	SVR	0.999 ± 0.003	1.1
image	KLR	1.011 ± 0.040	3.3	doppler	KRR	0.954 ± 0.051	1.3
image	SVM	1.030 ± 0.047	1.5	doppler	SVR	0.981 ± 0.010	1.1
ringnorm	KLR	0.963 ± 0.037	1.1	heavisine	KRR	0.990 ± 0.005	2.6
ringnorm	SVM	1.005 ± 0.013	1.0	heavisine	SVR	0.995 ± 0.003	6.9
splice	KLR	0.992 ± 0.020	1.6	kin	KRR	1.000 ± 0.003	6.8
splice	SVM	1.012 ± 0.014	1.1	kin	SVR	1.000 ± 0.000	3.8
twonorm	KLR	0.988 ± 0.029	0.9	pumadyn	KRR	1.003 ± 0.003	26.0
twonorm	SVM	1.001 ± 0.010	0.9	pumadyn	SVR	1.000 ± 0.001	18.4
waveform	KLR	0.997 ± 0.013	1.5	*Unpaired Version of CVST*			
waveform	SVM	1.011 ± 0.012	1.3				
banana	KLR	**1.056 ± 0.036**	0.7	bank	KRR	**1.073 ± 0.024**	0.6
banana	SVM	**1.106 ± 0.086**	0.3	bank	SVR	**1.006 ± 0.003**	0.7
covtype	KLR	**1.062 ± 0.028**	0.9	blocks	KRR	**1.428 ± 0.102**	0.7
covtype	SVM	**1.031 ± 0.020**	0.4	blocks	SVR	**1.189 ± 0.033**	0.7
german	KLR	**1.085 ± 0.031**	1.5	bumps	KRR	**1.947 ± 0.380**	0.7
german	SVM	**1.132 ± 0.061**	0.6	bumps	SVR	**1.049 ± 0.015**	0.7
image	KLR	**1.544 ± 0.185**	0.4	doppler	KRR	**1.896 ± 0.186**	0.7
image	SVM	**1.279 ± 0.143**	0.8	doppler	SVR	**1.210 ± 0.035**	0.7
ringnorm	KLR	**2.083 ± 0.291**	1.3	heavisine	KRR	**1.104 ± 0.022**	0.4
ringnorm	SVM	**1.044 ± 0.038**	0.5	heavisine	SVR	**1.042 ± 0.011**	0.5
splice	KLR	**1.106 ± 0.067**	0.6	kin	KRR	**1.074 ± 0.030**	0.3
splice	SVM	**1.092 ± 0.039**	0.6	kin	SVR	**1.014 ± 0.006**	0.7
twonorm	KLR	**1.197 ± 0.103**	0.7	pumadyn	KRR	**1.053 ± 0.016**	0.4
twonorm	SVM	**1.032 ± 0.026**	0.4	pumadyn	SVR	**1.026 ± 0.007**	0.4
waveform	KLR	**1.099 ± 0.036**	0.7	*Cross-Validation on 10% of Data*			
waveform	SVM	**1.088 ± 0.063**	0.4				
banana	KLR	**1.198 ± 0.131**	1.0	bank	KRR	**1.339 ± 0.068**	1.0
banana	SVM	0.970 ± 0.012	1.0	bank	SVR	**3.070 ± 0.376**	1.0
covtype	KLR	**1.185 ± 0.044**	1.0	blocks	KRR	**2.059 ± 0.529**	1.0
covtype	SVM	0.886 ± 0.032	1.0	blocks	SVR	**1.526 ± 0.314**	1.0
german	KLR	**1.128 ± 0.098**	1.0	bumps	KRR	**2.567 ± 0.629**	1.0
german	SVM	1.020 ± 0.024	1.0	bumps	SVR	**4.461 ± 0.511**	1.0
image	KLR	**2.188 ± 0.512**	1.0	doppler	KRR	**1.891 ± 0.405**	1.0
image	SVM	**1.133 ± 0.064**	1.0	doppler	SVR	**2.337 ± 0.583**	1.0
ringnorm	KLR	**5.972 ± 2.315**	1.0	heavisine	KRR	**1.075 ± 0.012**	1.0
ringnorm	SVM	0.648 ± 0.094	1.0	heavisine	SVR	1.012 ± 0.043	1.0
splice	KLR	**2.062 ± 0.389**	1.0	kin	KRR	**1.283 ± 0.049**	1.0
splice	SVM	0.874 ± 0.022	1.0	kin	SVR	**1.190 ± 0.033**	1.0
twonorm	KLR	2.427 ± 1.444	1.0	pumadyn	KRR	**1.113 ± 0.026**	1.0
twonorm	SVM	0.939 ± 0.027	1.0	pumadyn	SVR	**1.070 ± 0.025**	1.0
waveform	KLR	**2.032 ± 0.600**	1.0	*Random Search*			
waveform	SVM	0.959 ± 0.019	1.0				

Table 3: Comparison of performance of the CVST algorithm to different competitors (details see text). MSE ratio is the relative gain in MSE of CVST compared to the other variant. Speed denotes the relative speed increase of CVST compared to the other variant. We report the mean values over 50 repetitions and 1.96 standard errors with significant better values of CVST in boldface.

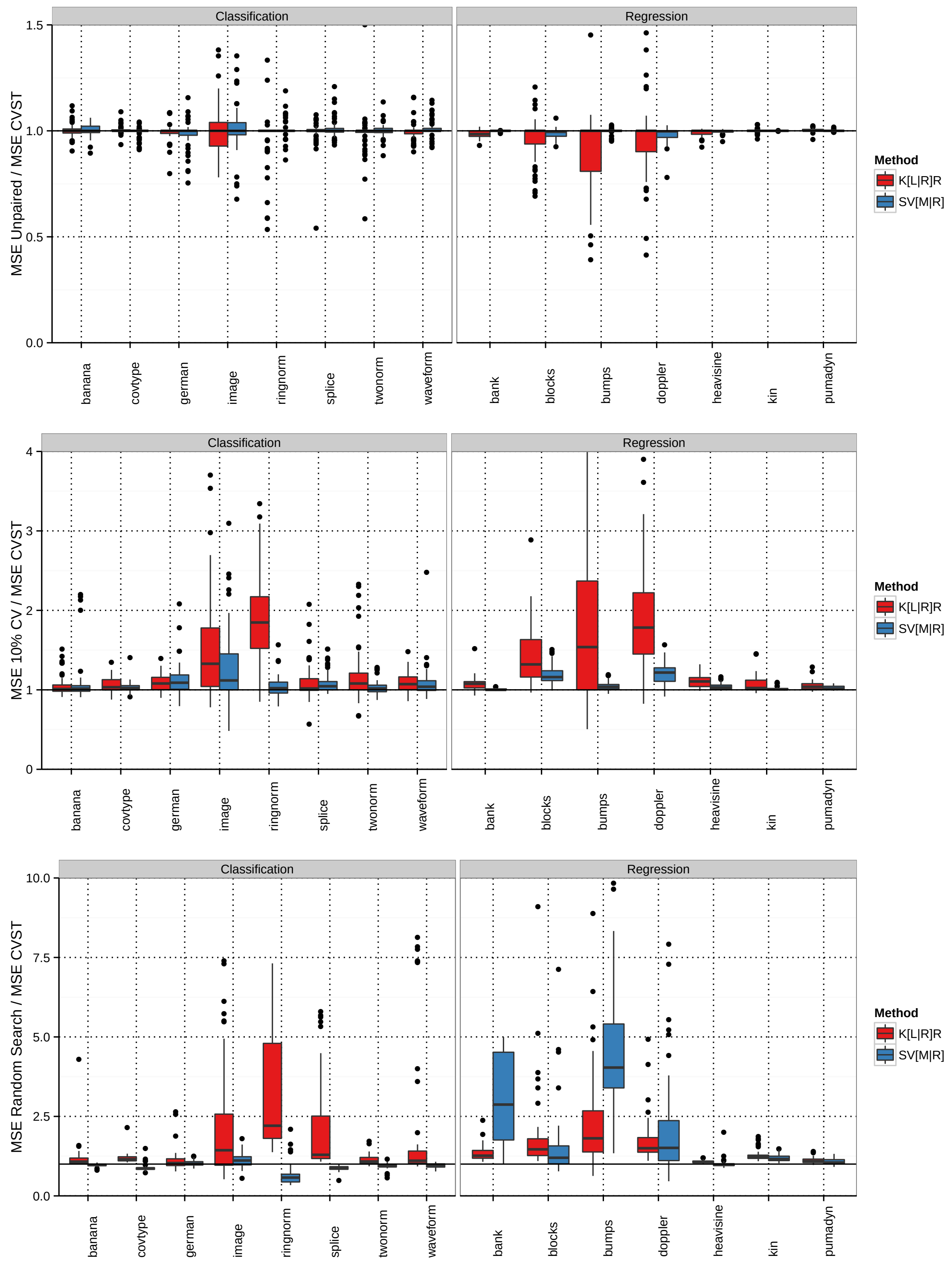

Figure 17: Distributions of the MSE ratio of the CVST procedure compared to the unpaired variant (upper panel), the cross-validation on 10% of the data (middle panel) and random search (lower panel). The horizontal line denotes the 1.0, i.e., equal performance ratio. Values over 1.0 favor the CVST procedure.

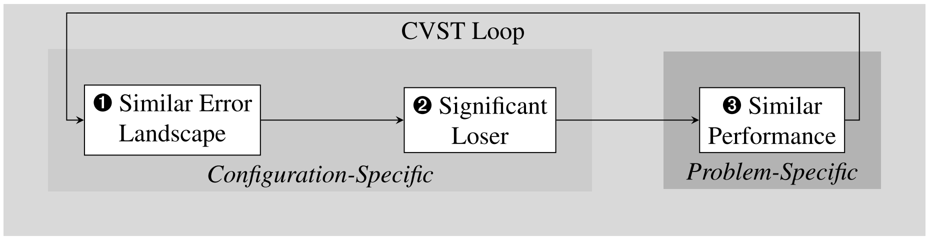

Figure 18: Conceptual view of the CVST algorithm. Each execution of the loop body consists of a sequence of test, each delivering the input for the following test. This modular structure allows for customization of the CVST algorithm to special situations (multi-class experiments, structured learning etc.).

is depicted in Figure 18: While the tests for top or flop configurations (step ❶) and the following sequential analysis (step ❷) focuses solely on the individual configurations, the early stopping rule (step ❸) acts on a global scope by determining the right point to stop the CVST algorithm. Thus, we face two kinds of test, namely the configuration-specific and the problem-specific tests.

To complete our discussion of the CVST algorithm, we focus on the configuration-specific procedures. First, we analyze the inner structure of the similarity test based on the error landscape in Section 7.1 and how this module can be adjusted for specific side constraints. Furthermore, in Section 7.2 we look at the suitability of the sequential analysis for determining significant loser configurations. It is shown that a so-called *closed* sequential test lacks essential properties of the open variant of Wald used in the CVST algorithm, which further underlines the appropriateness of the open test of Wald for the learning on increasing subsets of data.

7.1 Checking the Similarity of the Error Landscape

In the evaluation of the CVST method in Section 6 we see that the Friedman test for the regression case shows a much more aggressive behavior than the Cochran's Q test used in the top or flop conversion in the classification case. This feature can be clearly seen in Figure 16 where the dropping rates of the classification and regression benchmark data sets can be easily compared. Since the Friedman test acts on the squared residuals it uses more information compared to the classification task where we just have the information whether a specific data point was correctly classified or not. Thus, the Friedman test can exploit the higher detail of the information and can decide much faster than the Cochran's Q test which of the configurations are significantly different from the top performing ones.

In this section we show how the modular design of the CVST algorithm can be utilized to fit a less aggressive, yet more robust similarity test for regression data into the overall framework. It comes as no surprise that this increased tolerance affects the runtime of the CVST procedure. In the following we will first develop the alternative similarity test and then compare its performance both on the toy and the benchmark data sets to the original Friedman variant.

Recall from Section 4.1 that the top or flop assignment was calculated in a sequential manner: First we order all remaining configurations according to their mean performance; then we check at which point the addition of another configuration shows a significantly different behavior compared to all other, better performing configurations. To employ a less strict version of the Friedman test we drop the actual residual information and instead use the outlier behavior of a configuration for comparison. To this end we assume that the residuals are normally distributed with mean zero and a configuration-dependent variance σ_c^2 which we estimate from the actual residuals. Now we can check for each calculated residual whether it exceeds the $\frac{\alpha}{2}$ confidence interval around zero by using the normality assumption, thus converting the raw residuals in a binary information whether it is deemed as an outlier or not. Similar to the classification case this binary matrix forms the input to the Cochran's Q test which then asserts whether a specific configuration belongs to the top-performing ones or not.

The results of this procedure on the *noisy sinc* data set is shown in Figure 19: Compared to the outcome of the Friedman test in Figure 12 we can clearly see that the conservative nature of the outlier-based test helps in finding the correct parameter configuration. Obviously its higher retention rate leads to lower runtime performance: The speed ratio drops roughly by a factor of $\frac{2}{3}$. A similar behavior can be observed on the *benchmark* data sets in Figure 20: The conservative behavior of the outlier-based measure increases the MSE ratio compared to the residual-based test, but at the same time lowers the speed ratio. Interestingly, for the *benchmark* data sets the speed impact on the SVR is much lower compared to the speed ratio decrease of the KRR method. We can observe this shift also in the number of kept configurations shown in Figure 21 both for the *noisy sinc* and the *benchmark* data sets.

The conclusion of this discussion is two-fold: First, this section shows how the modular construction of the CVST methods allows for the exchange of the individual parts of the algorithm without disrupting the workflow of the procedure. If the residual-based test turns out to be unsuitable for a given regression problem, it is extremely easy to devise an adapted version for instance by looking at the outlier behavior of the configurations. Second, we see the inherent flexibility of the CVST algorithm. If there is a need for different error measures (for instance multi-class experiments, structured learning etc.), the modularized structure of the CVST algorithms allows for maximal flexibility and adaptability to special cases.

7.2 Determining Significant Losers: Open versus Closed Sequential Testing

As already introduced in Section 4.2 the sequential testing was pioneered by Wald (1947); the test monitors a likelihood ratio of a sequence of i.i.d. Bernoulli variables $B_1, B_2, \ldots$:

$$\ell = \prod_{i=1}^{n} f(b_i, \pi_1) / \prod_{i=1}^{n} f(b_i, \pi_0) \quad \text{given } H_h : B_i \sim \pi_h, h \in \{0, 1\}.$$

Hypothesis H_1 is accepted if $\ell \geq A$ and contrary H_0 is accepted if $\ell \leq B$. If neither of these conditions apply, the procedure cannot accept either of the two hypotheses and needs more data. A and B are chosen such that the error probability of the two decisions does not exceed α_l and β_l respectively. In Wald and Wolfowitz (1948) it is proven that the open sequential probability ratio test of Wald is optimal in the sense that compared to all tests

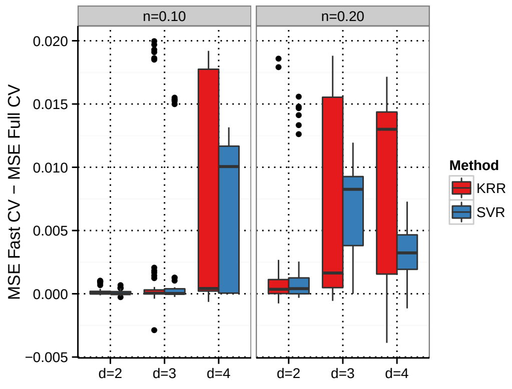

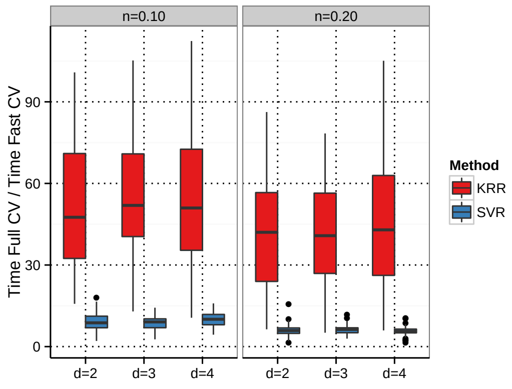

Figure 19: Difference in mean square error (left plots) and relative speed gain (right plots) for the *noisy sinc* data set using the outlier-based similarity test. In comparison to the stricter Friedman test used in Figure 12 we can observer a more conservative behavior resulting in increased robustness at the expense of performance.

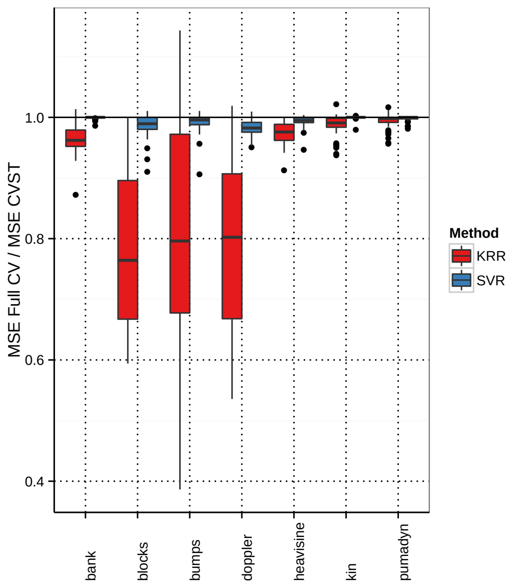

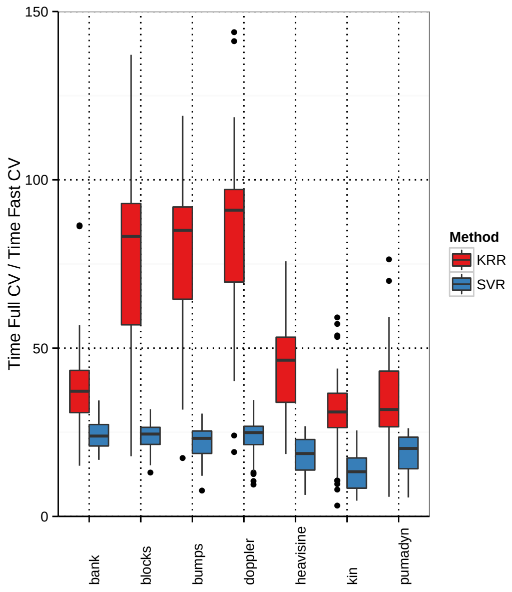

Figure 20: MSE ratio (left plot) and relative speed gain (right plot) for the *benchmark* data sets using the outlier-based similarity test. Compared to Figure 15 we can see better accuracy but decreased speed performance.

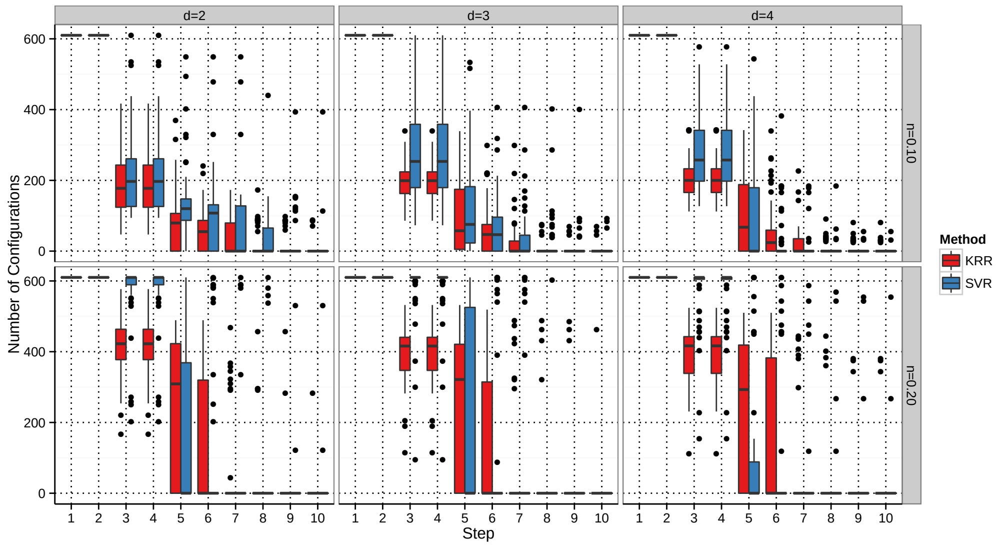

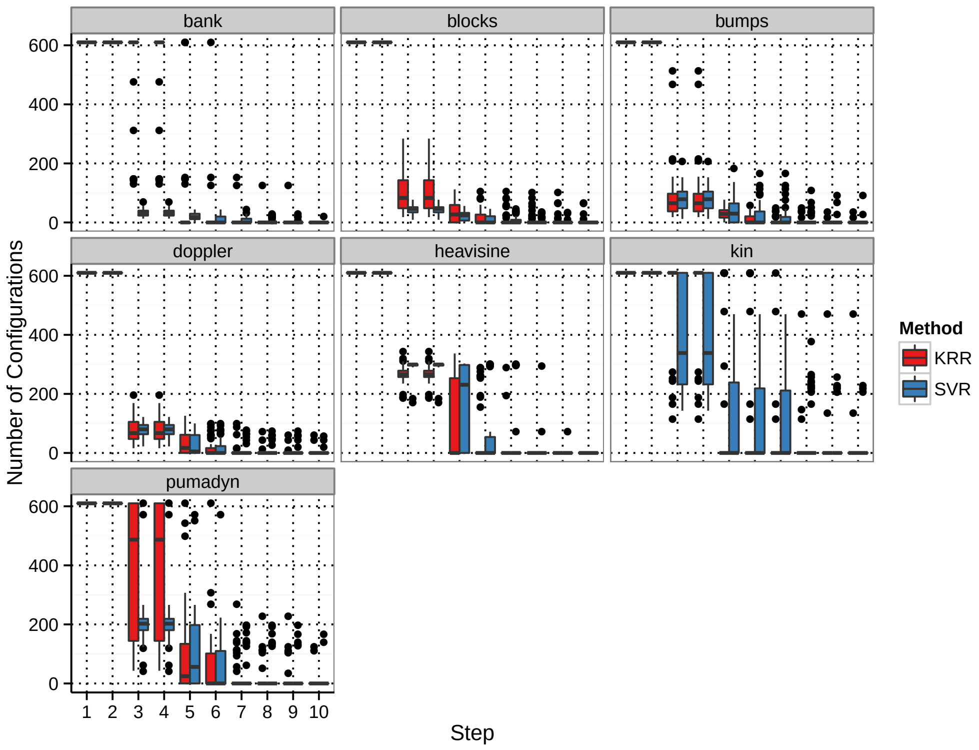

Figure 21: Remaining configurations after each step for the *noisy sinc* and different *benchmark* data sets using the outlier-based similarity test. Compared to Figure 13 and Figure 16 we can clearly observe the higher retention rate of this more conservative test.

with the same power it requires on average fewest observations for a decision. The testing scheme of Wald is called *open* since the procedure could potentially go on forever, as long as ℓ does not leave the (A, B)-tunnel.

The open design of Wald's procedure led to a development of a different kind of sequential tests, where the number of observations is fixed beforehand (see Armitage, 1960; Spicer, 1962; Alling, 1966; McPherson and Armitage, 1971). For instance in clinical studies it might be impossible or ethically prohibitive to use a test which potentially could go on forever. Unfortunately, none of these so-called closed tests exhibit an optimality criterion, therefore we choose one which at least in simulation studies showed the best behavior in terms of average sample number statistics: The method of Spicer (1962) is based on a gambler's ruin scenario in which both players have a fixed fortune and decide to play for n games. If $f(n, \pi, F_a, F_b)$ is the probability that a player with fortune F_a and stake b will ruin his opponent with fortune F_b in exactly n games, then the following recurrence holds:

$$f(n, \pi, F_a, F_b) = \begin{cases} 0 & \text{if } F_a < 0 \vee (n = 0 \wedge F_b > 0), \\ 1 & \text{if } n = 0 \wedge F_a > 0 \wedge F_b \leq 0, \\ \pi f(n-1, \pi, F_a + 1, F_b - b) & \\ \qquad +(1-\pi) f(n-1, \pi, F_a - b, F_b + b) & \text{otherwise.} \end{cases}$$

In each step, the player can either win a game with probability π and win 1 from his opponent or lose the stake b to the other player. Now, given $n = x + y$ games of which player A has won y and player B has won x, the game will stop if either of the following conditions hold:

$$y - bx = -F_a \Leftrightarrow y = \frac{b}{1+b} n - \frac{F_a}{1+b} \quad \text{or} \quad y - bx = F_b \Leftrightarrow y = \frac{b}{1+b} n - \frac{F_b}{1+b}.$$

This formulation casts the gambler's ruin problem into a Wald-like scheme, where we just observe the cumulative wins of player A and check whether we reached the lower or upper line. If we now choose F_a and F_b such that $f(n, 0.5, F_a, F_b) \leq \alpha_l$, we construct a test which allows us to check whether a given configuration performs worse than $\pi = 0.5$ (i.e., crosses the lower line) and can therefore be flagged as an overall loser with controlled error probability of α_l (see Alling 1966). For more details on the closed design of Spicer please consult Spicer (1962).

Since simulation studies show that the closed variants of the sequential testing exhibit low average sample number statistics, we first have a look at the runtime performance of the CVST algorithm equipped with either the open or the closed sequential test. The most influential parameter in terms of runtime is the S parameter. In principle, a larger number of steps leads to more robust estimates, but also to an increase of computation time. We study the effect of different choices of this parameter in a simulation. For the sake of simplicity we assume that the binary top or flop scheme consists of independent Bernoulli variables with $\pi_{\text{winner}} \in [0.9, 1.0]$ and $\pi_{\text{loser}} \in [0.0, 0.1]$. We test both the open and the closed sequential test and compare the relative speed-up of the CVST algorithm compared to a full 10-fold cross-validation in case the learner is cubic.

Figure 22 shows the resulting simulated runtimes for different settings. The overall speed-up is much higher for the closed sequential test indicating a more aggressive behavior

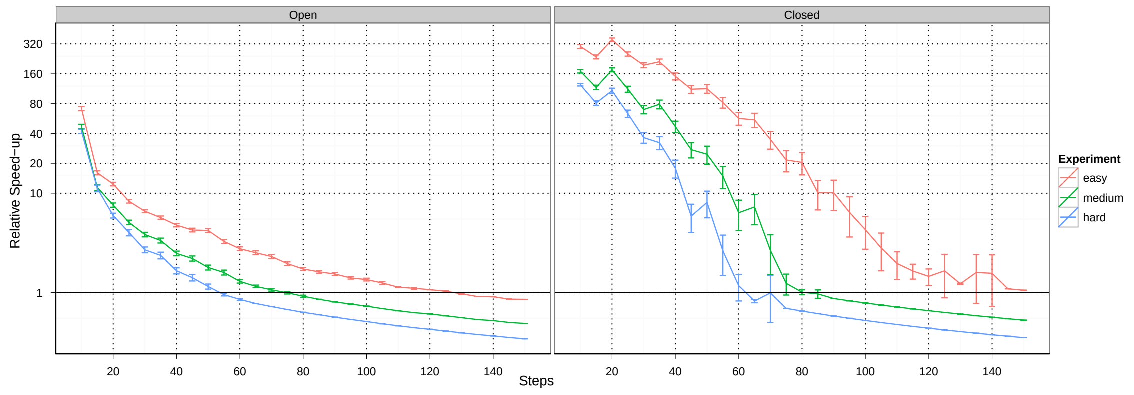

Figure 22: Relative speed gain of fast cross-validation compared to full cross-validation. We assume that training time is cubic in the number of samples. Shown are runtimes for 10-fold cross-validation on different problem classes by different loser/winner ratios (easy: 3:1; medium: 1:1, hard: 1:3) over 200 resamples.

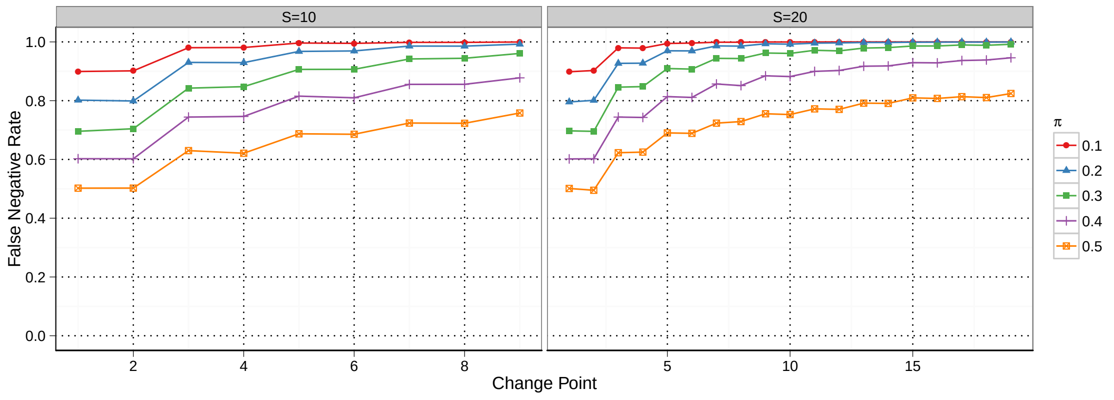

Figure 23: False negatives generated with the closed sequential test for non-stationary configurations, i.e., at the given change point the Bernoulli variable changes its π_{before} from the indicated value to 1.0.

compared to the more conservative open alternative. Both tests show their highest increase in the range of 10 to 20 steps with a rapid decline towards the higher step numbers. So in terms of speed the closed sequential test definitely beats the more conservative open test.

To evaluate the false negatives of the closed sequential test we simulate switching configurations by independent Bernoulli variables which change their success probability π from a chosen $\pi_{\text{before}} \in \{0.1, 0.2, \ldots, 0.5\}$ to a constant 1.0 at a given change point. By using this setup we mimic the behavior of a switching configuration which starts out as a loser and after enough data is available turns into a constant winner. The results can be seen in Figure 23 which reveals that the speed gain comes at a price: Apart from having no control over the safety zone, the number of falsely dropped configurations is much higher than for the open sequential test (see Figure 7 in Section 5.1). While having a definitive advantage over the open test in terms of speed, the false negative rate of the closed test renders it useless for the CVST algorithm.

8. Conclusion

We presented a method to speed up the cross-validation procedure by starting at subsets of the full training set size, identifying clearly underperforming parameter configurations early on and focusing on the most promising candidates for the larger subset sizes. We have discussed that taking subsets of the data set has theoretical advantages when compared to other heuristics like local search on the parameter set because the effects on the test errors are systematic and can be understood statistically. On the one hand, we argued that the optimal configurations converge to the true ones as sample sizes tend to infinity, but we also discussed in a concrete setting how the different behaviors of estimation error and approximation error lead to much faster convergence practically. These insights led to the introduction of a safety zone through sequential testing, which ensures that underperforming configurations are not removed prematurely when the minima are not converged yet. In experiments we showed that our procedure leads to a speed-up of up to 120 times compared to the full cross-validation without a significant increase in prediction error.

It will be interesting to combine this method with other procedures like the Hoeffding races or algorithms for multi-armed bandit problems. Furthermore, getting accurate convergence bounds even for finite sample size settings is another topic for future research.

Acknowledgments

We would like to acknowledge support for this project from the BMBF project ALICE, “Autonomous Learning in Complex Environments” (01IB10003B). We would like to thank Klaus-Robert Müller, Marius Kloft, Raphael Pelossof and Ralf Herbrich for fruitful discussions and help. We would also like to thank the anonymous reviewers who have helped to clarify a number of points and further improve the paper.

Appendix A. Sample-Size Independent Parametrization

In Section 2 we needed as a precondition that the test performances converge for a fixed parameter configuration c as n tends to infinity. In this section, we discuss this condition in the context of the empirical risk minimization. We refer to the book by Devroye et al. (1996) and the references contained therein for the theoretical results.

In the empirical risk minimization framework, a learning algorithm is interpreted as choosing the solution g_n with the best error on the training set $\hat{R}_n(g) = \frac{1}{n}\sum_{i=1}^{n} \ell(g(X_i), Y_i)$ from some hypothesis class $\mathcal{G}$. If the VC-dimension of $\mathcal{G}$, which roughly measures the complexity of $\mathcal{G}$, is finite then it holds that

$$\hat{R}_n(g) \to R(g)$$

uniformly over $g \in \mathcal{G}$, and consequently also $R(g_n) \to \inf_{g\in\mathcal{G}} R(g)$.

Now in order to make the link to our condition, we need that each parameter c corresponds to a fixed hypothesis class $\mathcal{G}_c$ (and not depend on the sample size in some way), and that the VC-dimension is finite. For feed-forward neural networks, one can show, for example, that neural networks with one hidden layer with k inner nodes and sigmoid activation function have finite VC-dimension (Devroye et al., 1996, Theorem 30.6).

For kernel machines, we consider the reproducing kernel Hilbert space (RKHS, Aronszajn 1950) view: Let $\mathcal{H}_k$ the RKHS induced by a Mercer kernel k with norm $\|\cdot\|_{\mathcal{H}_k}$. Evgeniou and Pontil (1999) show that the V_γ-dimension of the hypothesis class $\mathcal{G}(A) = \{f \in \mathcal{H}_k \mid \|f\|^2_{\mathcal{H}_k} \leq A\}$ is finite, from which uniform converges of the kind described above follows, and thus also that our condition holds.

Many kernel methods, including kernel ridge regression and support vector machines can be written as regularized optimization problems in the RKHS of the form:

$$\min_{f\in\mathcal{H}_k} \left(\frac{1}{n}\sum_{i=1}^{n} \ell(f(X_i), Y_i) + C\|f\|^2_{\mathcal{H}_k} \right) = \min_{f\in\mathcal{H}_k} \left(\hat{R}_n(f) + C\|f\|^2_{\mathcal{H}_k} \right).$$

Now if we assume that $\ell(f(x), y)$ is bounded by B and continuous in f, it follows that the minimum is attained for some f with $\|f\|^2_{\mathcal{H}_k} \leq B/C$: For $\|f\|_{\mathcal{H}_k} = 0$, $\hat{R}_n(f) + C\|f\|^2_{\mathcal{H}_k} \leq B$, and for $\|f\|_{\mathcal{H}_k} > B/C$, $\hat{R}_n(f) + C\|f\|^2_{\mathcal{H}_k} > B$. Because $\hat{R}(f) + C\|f\|^2_{\mathcal{H}_k}$ is continuous in f, it follows that the minimum is somewhere in-between.

Now $\hat{R}_n(f)$ converges to $R(f)$ uniformly over $f \in \mathcal{G}(B/C)$, such that there exists an $A \leq B/C$ such that

$$\min_{f\in\mathcal{H}_k} \left(\hat{R}(f) + C\|f\|^2_{\mathcal{H}_k} \right) = \min_{f\in\mathcal{G}(A)} R(f),$$

and we see that a regularization constant C corresponds to a fixed hypothesis class $\mathcal{G}(A)$ and our condition holds again.

As a direct consequence of this discussion we have to take care of the correct scaling of the regularization constants during the CVST run. Thus, for kernel ridge regression we have to scale the λ parameter linearly with the data set size and for the SVR divide the C parameter accordingly (see the reference implementation in the official CRAN package named `CVST` or the development version at `https://github.com/tammok/CVST` for details).

Appendix B. Example Run of CVST Algorithm

In this section we give an example of the whole CVST algorithm on one *noisy sinc* data set of $n = 1,000$ data points with intrinsic dimensionality of $d = 2$. The CVST algorithm is executed with $S = 10$ and $w_{\text{stop}} = 4$. We use a ν-SVM (Schölkopf et al., 2000) and test a parameter grid of $\log_{10}(\sigma) \in \{-3, -2.9, \ldots, 3\}$ and $\nu \in \{0.05, 0.1, \ldots, 0.5\}$. The procedure runs for 4 steps after which the early stopping rule takes effect. This yields the following traces matrix (only remaining configurations are shown):

	n = 90	**n = 180**	**n = 270**	**n = 360**
$\log_{10}(\sigma) = -2.3, \nu = 0.35$	0	0	1	0
$\log_{10}(\sigma) = -2.3, \nu = 0.40$	0	1	1	0
$\log_{10}(\sigma) = -2.3, \nu = 0.45$	0	1	0	1
$\log_{10}(\sigma) = -2.2, \nu = 0.30$	0	1	0	0
$\log_{10}(\sigma) = -2.2, \nu = 0.35$	0	1	1	0
$\log_{10}(\sigma) = -2.2, \nu = 0.40$	0	1	1	1
$\log_{10}(\sigma) = -2.2, \nu = 0.45$	0	1	1	1
$\log_{10}(\sigma) = -2.2, \nu = 0.50$	0	0	1	1
$\log_{10}(\sigma) = -2.1, \nu = 0.35$	0	1	1	1
$\log_{10}(\sigma) = -2.1, \nu = 0.40$	0	1	1	1
$\log_{10}(\sigma) = -2.1, \nu = 0.45$	0	1	1	1
$\log_{10}(\sigma) = -2.1, \nu = 0.50$	1	0	1	1
$\log_{10}(\sigma) = -2.0, \nu = 0.50$	0	0	1	1

The corresponding mean square errors of the remaining configurations after each step are shown in the next matrix. Based on these values, the winning configuration, namely $\log_{10}(\sigma) = -2.1, \nu = 0.40$ is chosen:

	n = 90	**n = 180**	**n = 270**	**n = 360**
$\log_{10}(\sigma) = -2.3, \nu = 0.35$	0.0370	0.0199	0.0145	0.0150
$\log_{10}(\sigma) = -2.3, \nu = 0.40$	0.0362	0.0197	0.0146	0.0146
$\log_{10}(\sigma) = -2.3, \nu = 0.45$	0.0356	0.0197	0.0146	0.0144
$\log_{10}(\sigma) = -2.2, \nu = 0.30$	0.0365	0.0195	0.0146	0.0148
$\log_{10}(\sigma) = -2.2, \nu = 0.35$	0.0351	0.0193	0.0142	0.0145
$\log_{10}(\sigma) = -2.2, \nu = 0.40$	0.0345	0.0194	0.0143	0.0141
$\log_{10}(\sigma) = -2.2, \nu = 0.45$	0.0340	0.0193	0.0143	0.0140
$\log_{10}(\sigma) = -2.2, \nu = 0.50$	0.0332	0.0200	0.0145	0.0138
$\log_{10}(\sigma) = -2.1, \nu = 0.35$	0.0353	0.0194	0.0144	0.0142
$\log_{10}(\sigma) = -2.1, \nu = 0.40$	0.0343	0.0195	0.0142	0.0138
$\log_{10}(\sigma) = -2.1, \nu = 0.45$	0.0340	0.0197	0.0140	0.0138
$\log_{10}(\sigma) = -2.1, \nu = 0.50$	0.0329	0.0199	0.0142	0.0137
$\log_{10}(\sigma) = -2.0, \nu = 0.50$	0.0351	0.0204	0.0145	0.0137

Appendix C. Nonparametric Tests

The tests used in the CVST algorithm are common tools in the field of statistical data analysis. Here we give a short summary based on Heckert and Filliben (2003) and cast the notation into the CVST framework context. Both methods deal with the performance matrix of K configurations with performance values on r data points:

	Data Points			
Configuration	1	2	...	r
1	x_{11}	x_{12}	...	x_{1r}
2	x_{21}	x_{22}	...	x_{2r}
3	x_{31}	x_{32}	...	x_{3r}
$\vdots$	$\vdots$	$\vdots$		$\vdots$
K	x_{K1}	x_{K2}	...	x_{Kr}

Both tests treat similar questions ("Do the K configurations have identical effects?") but are designed for different kinds of data: Cochran's Q test is tuned for binary x_{ij} while the Friedman test acts on continuous values. In the context of the CVST algorithm the tests are used for two different tasks:

1. Determine whether a set of configurations are the top performing ones (step ❶ in the overview Figure 3 and the function topConfigurations defined in Algorithm 2).

2. Check whether the remaining configurations behaved similar in the past (step ❸ in the overview Figure 3 and the function similarPerformance in Algorithm 4).

In both cases, the configurations are compared either by the performance on the samples (Point 1 above) or on the last w_{stop} traces (Point 2 above) of the remaining configurations. Depending on the learning problem either the Friedman test for regression task or the Cochran's Q test for classification tasks is used in Point 1.

In both cases the hypotheses for the tests are as follows:

- H_0: All configurations are equally effective (no effect)

- H_1: There is a difference in the effectiveness among the configurations, i.e., there is at least one configuration showing a significantly different effect on the data points.

C.1 Cochran's Q Test

The test statistic T is calculated as follows:

$$T = K(K-1)\frac{\sum_{i=1}^{K}(R_i - \frac{M}{K})^2}{\sum_{i=1}^{r} C_i(K - C_i)}$$

with R_i denoting the row total for the i^{th} configuration, C_i the column total for the i^{th} data point, and M the grand total. We reject H_0, if $T > \chi^2(1-\alpha, K-1)$ with $\chi^2(1-\alpha, K-1)$ denoting the $(1-\alpha)$-quantile of the χ^2 distribution with $K-1$ degrees of freedom and α is the significance level. As Cochran (1950) points out, the χ^2 approximation breaks down for small tables. Tate and Brown (1970) state that as long as the table contains at least 24 entries, the χ^2 approximation will suffice, otherwise the exact distribution should be used which can either be calculated explicitly (see Patil, 1975) or determined via permutation.

C.2 Friedman Test

Let $R(x_{ij})$ be the rank assigned to x_{ij} within data point i (i.e., rank of a configuration on data point i). Average ranks are used in the case of ties. The ranks for a configuration at position k are summed up over the data points to obtain

$$R_k = \sum_{i=1}^{r} R(x_{ki}).$$

The test statistic T is then calculated as follows:

$$T = \frac{12}{rK(K+1)} \sum_{i=1}^{K} (R_i - r(K+1)/2)^2.$$

If there are ties, then

$$T = \frac{(K-1)\sum_{i=1}^{K}(R_i - r(K+1)/2)^2}{[\sum_{i=1}^{K}\sum_{j=1}^{r} R(x_{ij})^2] - [rK(K+1)^2]/4}.$$

We reject H_0 if $T > \chi^2(\alpha, K-1)$ with $\chi^2(\alpha, K-1)$ denoting the α-quantile of the χ^2 distribution with $K-1$ degrees of freedom and α being the significance level.

Appendix D. Proof of Safety Zone Bound

In this section we prove the safety zone bound of Section 5.1 of the paper. We will follow the notation and treatment of the sequential analysis as found in the original publication of Wald (1947), Sections 5.3 to 5.5. First of all, Wald proves in Equation 5:27 that the following approximation holds:

$$\mathrm{ASN}(\pi_0, \pi_1 | \pi = 1.0) \approx \frac{\log \frac{1-\beta_l}{\alpha_l}}{\log \frac{\pi_1}{\pi_0}}.$$

where $\mathrm{ASN}(\cdot,\cdot)$ (Average Sample Number) is the expected number of steps until the given test will yield a decision, if the underlying success probability of the tested sequence is $\pi = 1.0$. The minimal $\mathrm{ASN}(\pi_0, \pi_1 | \pi = 1.0)$ is therefore attained if $\log \frac{\pi_1}{\pi_0}$ is maximal, which is clearly the case for $\pi_1 = 1.0$ and $\pi_0 = 0.5$, which holds by construction. So we get the lower bound of S for a given significance level α_l, β_l:

$$S \geq \left\lceil \log \frac{1-\beta_l}{\alpha_l} / \log 2 \right\rceil.$$

The lower line L_0 of the graphical sequential analysis test as exemplified in Figure 3 of the paper is defined as follows (see Equation 5:13 - 5:15):

$$L_0 = \frac{\log \frac{\beta_l}{1-\alpha_l}}{\log \frac{\pi_1}{\pi_0} - \log \frac{1-\pi_1}{1-\pi_0}} + n \frac{\log \frac{1-\pi_0}{1-\pi_1}}{\log \frac{\pi_1}{\pi_0} - \log \frac{1-\pi_1}{1-\pi_0}}.$$

Setting $L_0 = 0$, we can get the intersection of the lower test line with the x-axis and therefore the earliest step s_{safe}, in which the procedure will drop a constant loser configuration. This yields

$$s_{\text{safe}} = -\frac{\log \frac{\beta_l}{1-\alpha_l}}{\log \frac{\pi_1}{\pi_0} - \log \frac{1-\pi_1}{1-\pi_0}} \Big/ \frac{\log \frac{1-\pi_0}{1-\pi_1}}{\log \frac{\pi_1}{\pi_0} - \log \frac{1-\pi_1}{1-\pi_0}} = -\frac{\log \frac{\beta_l}{1-\alpha_l}}{\log \frac{1-\pi_0}{1-\pi_1}} = \frac{\log \frac{\beta_l}{1-\alpha_l}}{\log \frac{1-\pi_1}{1-\pi_0}} = \frac{\log \frac{\beta_l}{1-\alpha_l}}{\log 2 - \sqrt[S]{\frac{1-\beta_l}{\alpha_l}}}.$$

The last equality can be derived by inserting the closed form of π_1 given $\pi_0 = 0.5$:

$$S = \text{ASN}(\pi_0, \pi_1 | \pi = 1.0) = \frac{\log \frac{1-\beta_l}{\alpha_l}}{\log \frac{\pi_1}{\pi_0}} = \frac{\log \frac{1-\beta_l}{\alpha_l}}{\log 2\pi_1} \Leftrightarrow 2\pi_1 = \sqrt[S]{\frac{1-\beta_l}{\alpha_l}} \Leftrightarrow \pi_1 = \frac{1}{2}\sqrt[S]{\frac{1-\beta_l}{\alpha_l}}.$$

Setting s_{safe} in relation to the maximal number of steps S yields the safety zone bound of Section 5.1.

Appendix E. Proof of Computational Budget

For the size N of the whole data set and a learner of time complexity $f(n) = n^m$, where $m \in \mathbb{N}$, resulting in a learning time of $t = N^m$, one observes that learning on a proportion of size $\frac{i}{S}N$ takes about $\frac{i^m}{S^m}t$ time. By construction one has to learn on all K parameter configurations in each step before hitting $s_r \times S$ and on $K \times r$ parameter configurations with drop rate $(1-r)$ afterwards. Thus the entirely needed computation time is given by

$$K \times (1-r) \sum_{i=1}^{s_r \times S} \frac{i^m}{S^m} t + K \times r \sum_{i=1}^{S} \frac{i^m}{S^m} t$$

which should be smaller than the given time budget T.

Making use of the fact proved in Appendix E.1 that $\frac{1}{n^{m-1}} \sum_{i=1}^{n} i^m \dot{\leq} \frac{n^2}{m+1} + \frac{n}{2} + \frac{m}{12}$ holds under the mild condition of $n > \frac{m}{2\pi}$, where $\dot{\leq}$ describes an asymptotic relation, one can reformulate the inequality as follows:

$$\begin{aligned} &\frac{tK(1-r)s_r^{m-1}}{S} \frac{1}{(s_r S)^{m-1}} \sum_{i=1}^{s_r S} i^m + \frac{tKr}{S} \frac{1}{S^{m-1}} \sum_{i=1}^{S} i^m \\ &\dot{\leq} \frac{tK}{S} \left[(1-r)s_r^{m-1} \left(\frac{(s_r S)^2}{m+1} + \frac{s_r S}{2} + \frac{m}{12} \right) + r \left(\frac{S^2}{m+1} + \frac{S}{2} + \frac{m}{12} \right) \right] \dot{\leq} T. \end{aligned}$$

It is obvious that this inequality is quadratic in the variable S which can be solved by bringing the above inequality in standard form:

$$\begin{aligned} & 0 \dot{\geq} \left[(1-r)s_r^{m-1} \left(\frac{(s_r S)^2}{m+1} + \frac{s_r S}{2} + \frac{m}{12} \right) + r \left(\frac{S^2}{m+1} + \frac{S}{2} + \frac{m}{12} \right) \right] - \frac{TS}{tK} \\ \Leftrightarrow\ & 0 \dot{\geq} \frac{(1-r)s_r^{m+1} + r}{m+1} S^2 + \left[\frac{(1-r)s_r^m + r}{2} - \frac{T}{tK} \right] S + \left((1-r)s_r^{m-1} + r \right) \frac{m}{12} \\ \Leftrightarrow\ & 0 \dot{\geq} S^2 + 2 \left[\frac{m+1}{4} \frac{tK(1-r)s_r^m + tKr - 2T}{((1-r)s_r^{m+1} + r)tK} \right] S + \frac{m(m+1)}{12} \frac{(1-r)s_r^{m-1} + r}{(1-r)s_r^{m+1} + r}. \end{aligned}$$

Substituting $a = \frac{m+1}{4}\frac{tK(1-r)s_r^m + tKr - 2T}{((1-r)s_r^{m+1}+r)tK}$ and $b = \frac{m(m+1)}{12}\frac{(1-r)s_r^{m-1}+r}{(1-r)s_r^{m+1}+r}$ above is equivalent to:

$$S = -a + y,\, y \in \left\{-\sqrt{a^2-b}, +\sqrt{a^2-b}\right\}.$$

For the sake of a meaningful step amount, i.e., $S > 0$ and furthermore S as large as possible we choose it as

$$S = \left\lfloor -a + \sqrt{a^2-b} \right\rfloor.$$

Note that S is a function of the parameter s_r. The mild condition for the upper bound of power sums mentioned above has to be fulfilled. Since obviously $b \geq 0$ holds, a must be negative in order to gain a positive step amount. Furthermore the root has to be solvable. So the following constraints on s_r have to be made:

$$\begin{aligned} &(1) \qquad 2T \geq tK(1-r)s_r^m + tKr \\ &(2) \qquad a^2 \geq b \\ &(3) \qquad s_r S > \frac{m}{2\pi}. \end{aligned}$$

Note that condition (3) is trivial for a small degree of complexity m, which is the common case.

E.1 Proof of the Upper Bound

Assume that $n = \frac{m}{c}$ where $c < 2\pi$. Denote by B_i the *Bernoulli* numbers.

$$\begin{aligned} \frac{1}{n^{m-1}}\sum_{i=1}^{n} i^m &= \frac{1}{n^{m-1}}\Big[\frac{n^m}{2} + \frac{1}{m+1}\sum_{k=0}^{\lfloor \frac{m}{2} \rfloor}\binom{m+1}{2k}B_{2k}n^{m+1-2k}\Big] \\ &= \frac{n^2}{m+1} + \frac{n}{2} + \frac{m}{12} + \sum_{k=2}^{\lfloor \frac{m}{2} \rfloor}(-1)^{i+1}\frac{1}{m+1}\binom{m+1}{2k}|B_{2k}|n^{2-2k} \end{aligned}$$

The sum term is alternating in sign and asymptotically monotone decreasing in k:

$$\begin{aligned} \frac{1}{m+1}\binom{m+1}{2k}|B_{2k}|n^{2-2k} &\sim \frac{m!}{(2k)!(m+1-2k)!}2\frac{(2k)!}{(2\pi)^{2k}}\left(\frac{m}{c}\right)^{2-2k} \\ &= \frac{2m}{c^2}\underbrace{\prod_{j=0}^{2k-2}\left(1-\frac{j}{m}\right)}_{\downarrow 0 \; as \; k \to \infty}\underbrace{\left(\frac{c}{2\pi}\right)^{2k}}_{\downarrow 0 \,,\, \frac{c}{2\pi} < 1} \end{aligned}$$

where we use the asymptotic behavior of $|B_{2k}| \sim 2\frac{(2k)!}{(2\pi)^{2k}}$. Now that the sequence under the sum starts negative, grouping up each two subsequent elements gives a negative value, such that the sum also is negative.

Therefore

$$\frac{1}{n^{m-1}}\sum_{i=1}^{n} i^m \stackrel{\cdot}{\leq} \frac{n^2}{m+1} + \frac{n}{2} + \frac{m}{12}.$$

References

D. W. Alling. Closed sequential tests for binomial probabilities. *Biometrika*, 53(1/2):73–84, 1966.

S. Arlot, A. Celisse, and P. Painleve. A survey of cross-validation procedures for model selection. *Statistics Surveys*, 4:40–79, 2010.

P. Armitage. *Sequential Medical Trials.* Blackwell Scientific Publications, 1960.

N. Aronszajn. Theory of reproducing kernels. *Transactions of the American Mathematical Society*, 68:337–404, 1950.

P. L. Bartlett, P. M. Long, and R. C. Williamson. Fat-shattering and the learnability of real-valued functions. *Journal of Computer and Systems Science*, 52:434–452, 1996.

Y. Bengio. Gradient-based optimization of hyperparameters. *Neural Computation*, 12(8): 1889–1900, 2000.

J. Bergstra and Y. Bengio. Random search for hyper-parameter optimization. *Journal of Machine Learning Research*, 13:281–305, March 2012.

J. Bergstra, R. Bardenet, Y. Bengio, and B. Kégl. Algorithms for hyper-parameter optimization. In *Advances in Neural Information Processing Systems 24*, pages 2546–2554, 2011.

D. Berry and B. Fristedt. *Bandit problems: Sequential Allocation of Experiments.* Chapman & Hall, 1985.

M. Birattari. *Tuning Metaheuristics: A Machine Learning Perspective.* Springer, 2009.

M. Birattari, T. Stützle, L. Paquete, and K. Varrentrapp. A racing algorithm for configuring metaheuristics. In *Proceedings of the Genetic and Evolutionary Computation Conference*, pages 11–18, 2002.

J. A. Blackard and D. J. Dean. Comparative accuracies of artificial neural networks and discriminant analysis in predicting forest cover types from cartographic variables. *Computers and Electronics in Agriculture*, 24:131–151, 1999.

J. K. Bradley and R. Schapire. Filterboost: Regression and classification on large datasets. In *Advances in Neural Information Processing Systems 20*, pages 185–192, 2008.

M. L. Braun, J. Buhmann, and K.-R. Müller. On relevant dimensions in kernel feature spaces. *Journal of Machine Learning Research*, 9:1875–1908, 2008.

N. Cesa-Bianchi and G. Lugosi. *Prediction, Learning, and Games.* Cambridge University Press, 2006.

S. Chien, J. Gratch, and M. Burl. On the efficient allocation of resources for hypothesis evaluation: A statistical approach. *IEEE Transactions Pattern Analysis and Machine Intelligence*, 17:652–665, 1995.

S. Chien, A. Stechert, and D. Mutz. Efficient heuristic hypothesis ranking. *Journal of Artificial Intelligence Research*, 10:375–397, 1999.

W. G. Cochran. The comparison of percentages in matched samples. *Biometrika*, 37(3-4): 256–266, 1950.

L. Devroye, L. Györfi, and G. Lugosi. *A Probabilistic Theory of Pattern Recognition.* Springer, 1996.

P. Domingos and G. Hulten. A general method for scaling up machine learning algorithms and its application to clustering. In *Proceedings of the Eighteenth International Conference on Machine Learning*, pages 106–113, 2001.

D. L. Donoho and J. M. Johnstone. Ideal spatial adaptation by wavelet shrinkage. *Biometrika*, 81(3):425–455, 1994.

T. Evgeniou and M. Pontil. On the V gamma dimension for regression in reproducing kernel hilbert spaces. In O. Watanabe and T. Yokomori, editors, *Algorithmic Learning Theory*, pages 106–117, 1999.

M. Friedman. The use of ranks to avoid the assumption of normality implicit in the analysis of variance. *Journal of the American Statistical Association*, 32(200):675–701, 1937.

S. Geisser. The predictive sample reuse method with applications. *Journal of the American Statistical Association*, 70(350):320–328, 1975.

N. A. Heckert and J. J. Filliben. *NIST Handbook 148: DATAPLOT Reference Manual, Volume I: Commands.* National Institute of Standards and Technology Handbook Series, 2003.

V. Heidrich-Meisner and C. Igel. Hoeffding and Bernstein races for selecting policies in evolutionary direct policy search. In *Proceedings of the 26th Annual International Conference on Machine Learning*, pages 401–408, 2009.

S. S. Keerthi, V. Sindhwani, and O. Chapelle. An efficient method for gradient-based adaptation of hyperparameters in SVM models. In *Advances in Neural Information Processing Systems 19*, pages 673–680, 2006.

R. Kohavi and G. H. John. Automatic parameter selection by minimizing estimated error. In *Proceedings of the Twelfth International Conference on Machine Learning*, pages 304–312, 1995.

W. H. Kruskal and W. A. Wallis. Probable inference, the law of succession, and statistical inference. *Journal of the American Statistical Association*, 47(260):583–621, 1952.

O. Maron and A. W. Moore. Hoeffding races: Accelerating model selection search for classification and function approximation. In *Advances in Neural Information Processing Systems 6*, pages 59–66, 1994.

O. Maron and A. W. Moore. The racing algorithm: Model selection for lazy learners. *Artificial Intelligence Review*, 11:193–225, 1997.

C. K. McPherson and P. Armitage. Repeated significance tests on accumulating data when the null hypothesis is not true. *Journal of the Royal Statistical Society. Series A*, 134(1): 15–25, 1971.

V. Mnih, C. Szepesvári, and J.-Y. Audibert. Empirical Bernstein stopping. In *Proceedings of the 25th International Conference on Machine learning*, ICML '08, pages 672–679, 2008.

M. Mohri, A. Rostamizadeh, and A. Talwalkar. *Foundations Of Machine Learning.* MIT Press, 2012.

F. Mosteller and J. W. Tukey. *Handbook of Social Psychology*, volume 2, chapter Data analysis, including statistics, pages 80–203. Addison-Wesley, 2nd edition, 1968.

K. D. Patil. Cochran's Q test: Exact distribution. *Journal of the American Statistical Association*, 70(349):186–189, 1975.

R. Pelossof and M. Jones. Curtailed online boosting. Technical report, Columbia University, 2009.

R. Pelossof and Z. Ying. The attentive perceptron. *Computing Research Repository*, abs/1009.5972, 2010.

R. Pelossof and Z. Ying. Rapid learning with stochastic focus of attention. *Computing Research Repository*, abs/1105.0382, 2011.

G. Rätsch, T. Onoda, and K.-R. Müller. Soft margins for AdaBoost. *Machine Learning*, 42 (3):287–320, 2001.

V. Roth. Probabilistic discriminative kernel classifiers for multi-class problems. In *Proceedings of the 23rd DAGM-Symposium on Pattern Recognition*, pages 246–253, 2001.

B. Schölkopf, A. J. Smola, R. C. Williamson, and P. L. Bartlett. New support vector algorithms. *Neural Computation*, 12:1207–1245, 2000.

S. Smale and D.-X. Zhou. Estimating the approximation error in learning theory. *Analysis and Applications*, 1(1):1–25, 2003.

J. Snoek, H. Larochelle, and R. P. Adams. Practical bayesian optimization of machine learning algorithms. In *Advances in Neural Information Processing Systems 25*, pages 2960–2968, 2012.

C. C. Spicer. Some new closed sequential designs for clinical trials. *Biometrics*, 18(2): 203–211, 1962.

A. Stanski. *Konstruktives Probabilistisches Lernen.* PhD thesis, Technische Universität Berlin, 2012.

I. Steinwart and C. Scovel. Fast rates for support vector machines using Gaussian kernels. *Annals of Statistics*, 35:575–607, 2007.

M. Stone. Cross-validatory choice and assessment of statistical predictions. *Journal of the Royal Statistical Society. Series B*, 36(2):111–147, 1974.

M. W. Tate and S. M. Brown. Note on the Cochran Q test. *Journal of the American Statistical Association*, 65(329):155–160, 1970.

C. Thornton, F. Hutter, H. H. Hoos, and K. Leyton-Brown. Auto-WEKA: Automated selection and hyper-parameter optimization of classification algorithms. *CoRR*, abs/1208.3719, 2012.

V. Vapnik. *Statistical Learning Theory.* Wiley, 1998.

A. Wald. *Sequential Analysis.* Wiley, 1947.

A. Wald and J. Wolfowitz. Optimum character of the sequential probability ratio test. *The Annals of Mathematical Statistics*, 19(3):326–339, 1948.

G. B. Wetherill and K. D. Glazebrook. *Sequential Methods in Statistics.* Chapman and Hall, 1986.

E. B. Wilson. Probable inference, the law of succession, and statistical inference. *Journal of the American Statistical Association*, 22(158):209–212, 1927.

A. X. Zheng and M. Bilenko. Lazy paired hyper-parameter tuning. In *Proceedings of the 23rd International Joint Conference on Artificial Intelligence*, pages 1924–1931, 2013.